Water Resources Research

RESEARCH ARTICLE
10.1029/2021WR031289

Special Section:
Advancing process representation in hydrologic models: Integrating new concepts, knowledge, and data

From Dynamic Groundwater Level Measurements to Regional Aquifer Parameters— Assessing the Power of Spectral Analysis

Timo Houben[1,2], Estanislao Pujades[3], Thomas Kalbacher[4], Peter Dietrich[5,6], and Sabine Attinger[1,2]

[1]Department of Computational Hydrosystems, Helmholtz Centre for Environmental Research - UFZ, Leipzig, Germany, [2]Institute of Environmental Science and Geography, University of Potsdam, Potsdam, Germany, [3]Institute of Environmental Assessment and Water Research (IDAEA), Severo Ochoa Excellence Center of the Spanish Council for Scientific Research (CSIC), Barcelona, Spain, [4]Department of Environmental Informatics, Helmholtz Centre for Environmental Research - UFZ, Leipzig, Germany, [5]Department of Monitoring and Exploration Technologies, Helmholtz Centre for Environmental Research - UFZ, Leipzig, Germany, [6]Center for Applied Geoscience, University of Tübingen, Tübingen, Germany

Abstract Large-scale groundwater models are required to estimate groundwater availability and to inform water management strategies on the national scale. However, parameterization of large-scale groundwater models covering areas of major river basins and more is challenging due to the lack of observational data and the mismatch between the scales of modeling and measurements. In this work, we propose to bridge the scale gap and derive regional hydraulic parameters by spectral analysis of groundwater level fluctuations. We hypothesize that specific locations in aquifers can reveal regional parameters of the hydraulic system. We first generate ensembles of synthetic but realistic aquifers which systematically differ in complexity. Applying Liang and Zhang's (2013), https://doi.org/10.1016/j.jhydrol.2012.11.044, semi-analytical solution for the spectrum of hydraulic head time series, we identify for each ensemble member and at different locations representative aquifer parameters. Next, we extend our study to investigate the use of spectral analysis in more complex numerical models and in real settings. Our analyses indicate that the variance of inferred effective transmissivity and storativity values for stochastic aquifer ensembles is small for observation points which are far away from the Dirichlet boundary. Moreover, the head time series has to cover a period which is roughly 10 times as long as the characteristic time of the aquifer. In deterministic aquifer models we infer equivalent, regionally valid parameters. A sensitivity analysis further reveals that as long as the aquifer length and the position of the groundwater measurement location is roughly known, the parameters can be robustly estimated.

Plain Language Summary We build large-scale (regional) computer models of the subsurface flow conditions in order to quantify the long-term shift in groundwater storage and response on the national level under changing climatic conditions and increasing human water demands. These models must be fed with hydrogeological parameters obtained from subsurface observation wells, drilling logs, and hydraulic tests in conjunction with (hydro)geological and geostatistical methods. In some regions these wells are sparsely distributed and derived parameters are representative only for small areas. We hypothesize that groundwater level records can reveal regional aquifer information when analyzed in the spectral domain. In order to bridge that scale gap and because groundwater level time series are generally available, we propose to infer regional parameters by analyzing the frequency content (spectrum) of long groundwater level time series. The required parameters were determined using mathematical formulations of the theoretical spectrum for simplified settings. We tested the methodology in computer models with limited complexity and found that the groundwater level time series indeed contain regional information if the time of observation is sufficiently long. Lastly, we apply the spectral analysis to real groundwater data to test the capability of the method to infer regional aquifer parameters in real aquifers.

Key Points:

- We successfully tested the spectral analysis of groundwater level fluctuations in numerical models and obtained regional aquifer parameters
- In a sensitivity analysis of the spectral analysis using field data, the storativity and the response times could be robustly estimated
- The application of the suggested methodology to the field data from a catchment in central Germany produced plausible results

Supporting Information:

Supporting Information may be found in the online version of this article.

Correspondence to:

Timo Houben,
timo.houben@ufz.de

Citation:

Houben, T., Pujades, E., Kalbacher, T., Dietrich, P., & Attinger, S. (2022). From dynamic groundwater level measurements to regional aquifer parameters— Assessing the power of spectral analysis. *Water Resources Research*, *58*, e2021WR031289. https://doi.org/10.1029/2021WR031289

Received 24 SEP 2021
Accepted 9 MAY 2022

Author Contributions:

Conceptualization: Timo Houben, Estanislao Pujades, Thomas Kalbacher, Peter Dietrich, Sabine Attinger
Data curation: Timo Houben
Formal analysis: Timo Houben, Thomas Kalbacher, Peter Dietrich, Sabine Attinger

1. Introduction

The largest part of Earth's unbound fresh water is groundwater, thus being of great importance for human kind. Climate change is anticipated to have severe impacts on the amount and dynamics of groundwater recharge and consequently on water resources stored in aquifers (Butler et al., 2021; Russo & Lall, 2017; Whittemore et al., 2015). In particular, the spatial and temporal variations of the storage are still unclear. Furthermore, abstraction rates may increase to meet future human water demands, placing additional stress on groundwater

Funding acquisition: Thomas Kalbacher, Peter Dietrich, Sabine Attinger
Investigation: Timo Houben, Estanislao Pujades, Peter Dietrich, Sabine Attinger
Methodology: Timo Houben, Estanislao Pujades, Thomas Kalbacher, Peter Dietrich, Sabine Attinger
Software: Timo Houben, Thomas Kalbacher
Supervision: Estanislao Pujades, Thomas Kalbacher, Peter Dietrich, Sabine Attinger
Validation: Timo Houben, Peter Dietrich
Visualization: Timo Houben
Writing – original draft: Timo Houben, Sabine Attinger
Writing – review & editing: Timo Houben, Estanislao Pujades, Thomas Kalbacher, Peter Dietrich, Sabine Attinger

systems. Hydrological models are essential tools for describing and understanding the dynamics of hydrological systems, investigating the impact of climate and anthropogenically induced changes and lay the foundation to answer questions societies and decision makers face: How long do aquifers meet increasing water demands or buffer recharge fluctuations until groundwater levels fall and baseflows run dry? In order to answer these questions usually regional scale integrated models are established. The models often cover areas on the order of major river basins as the impact of climate change and human interventions affect hydrological processes operating at these scales. Regional groundwater models are then a part of these integrated hydrologic models, in which the representation of groundwater is usually conceptualized through simple linear reservoir approaches (e.g., Hamman et al., 2018; Samaniego et al., 2010; Sutanudjaja et al., 2018). In the last years, however, one can observe that more complex partial differential equation (PDE) based modeling approaches solving the spatially resolved groundwater flow equation are incorporated into or coupled with the codes as well (e.g., Hellwig et al., 2020; Jing et al., 2018; Markstrom et al., 2005; Maxwell & Miller, 2005; Srivastava et al., 2014; Sutanudjaja et al., 2011). The construction of regional PDE based groundwater models poses specific problems due to limited groundwater data availability but also due to the coarse numerical discretization of regional groundwater models. The standard procedure of building a PDE based groundwater model is composed of several steps. First, a structural geological model is established to describe the spatial geometry of the groundwater system which typically consists of different complex hydrogeological layers and facies. The extent and thickness of the relevant hydrogeological facies determine the capacity of the groundwater system to store and the ability to transmit groundwater. An appropriate estimation of the extent and thickness of layers and their complex connections is difficult to achieve. Consequently, the complex interplay of adjacent units which collectively contribute to regional groundwater behavior was often disregarded and replaced by a simpler conceptualization. In a second step, local groundwater level measurements and in-situ investigations such as pumping, slug test, or direct-push (e.g., Butler et al., 2007; Dietrich & Leven, 2009) together with laboratory experiments are used to infer hydraulic properties of the layers and facies and to delineate different hydrogeological units. However, all these measurements and data are rare in regional systems. Consequently, they cover only a small fraction of the whole aquifer system. In particular, since hydraulic properties of aquifers vary spatially over several orders of magnitude within an aquifer, rare measurements do not capture the heterogeneity of the system to its full extent. In addition, hydraulic tests and similar techniques predominantly describe local hydraulic properties of a groundwater system. Similarly, the absolute values of groundwater level measurements display very local conditions. Unfortunately, the support volume of these measurements does not match the discretization volumes of regional groundwater model which are usually much larger and in the order of several hundred meters. Installing many more groundwater monitoring wells is not feasible. The challenging question therefore is: are there alternative techniques for interpreting available but scarce groundwater data? An alternative approach might be developed from the following concept: Natural groundwater recharge is continuously and regionally forcing shallow aquifer systems like a continuous large scale injection test and aquifer systems are responding to it by changes in groundwater levels. Around 20 years ago, Zhang and colleagues studied the frequency distribution of groundwater level fluctuations (Zhang & Schilling, 2004) together with the frequency distribution of stream and baseflow fluctuations (Zhang & Li, 2005; Zhang & Schilling, 2005). They found that regional shallow aquifers transmit and alter the forcing signal in a specific way: Aquifers transforms the incoming signal into a signal in which frequencies higher than a specific cut-off frequency are attenuated. In other words, aquifers act as low-pass filters. Moreover, the cut-off frequency strongly depends on the aquifer properties like transmissivity, storativity, and spatial extension of the system. Therefore, the investigation of frequency distributions of groundwater level fluctuations may be used for parameter inversion. In addition, Zhang and colleagues found in their field studies but also in numerical simulations that the cut-off frequency is not very sensitive to local variations in the hydraulic conductivity. This raises the hypothesis that the cut-off frequency is dominated by regional and representative (Sanchez-Vila et al., 2006) hydraulic properties of aquifer systems and thus may be a suitable property to identify regional scale aquifer parameters.

Calculating the spectrum of a signal is a standard method to investigate the frequency distribution of time series. Pioneering work in the field of spectral analyses of groundwater systems has been conducted by Gelhar (1974). He developed analytical solutions in the frequency domain to describe the spectral response characteristics of three different ideal phreatic aquifers (linear reservoir, linear Dupuit aquifer, and Laplace aquifer) with time-variable recharge and river stage fluctuations. Similarly, Zhang and Schilling (2004) investigated a simple groundwater model forced by uncorrelated white noise recharge. They expanded their approach in subsequent studies and included the impact of temporally correlated recharge (Zhang & Li, 2006), spatial heterogeneity, and temporally

changing river stage on groundwater level fluctuations (Zhang & Yang, 2010) making use of non-stationary spectral analysis and numerical simulations.

Recently, researchers investigated the spectral response of hydrological systems and extended existing models in order to improve the quality of parameter determination (Schuite et al., 2019) or to estimate the impact of groundwater abstraction on groundwater levels (Condon & Maxwell, 2014). Moreover, Liang and Zhang (2013) presented an analytical solution of the hydraulic head spectrum for a bounded unconfined aquifer based on the linearized Boussinesq equation (Bear, 1972). The equation relates the recharge spectrum (input spectrum) to the head spectrum (output spectrum). Assuming stationarity in the time series, the relation between input and output can be expressed in terms of a transfer function which depends on the hydraulic parameters, the storativity, and the transmissivity. Transfer functions in general are also the focus of papers by Molénat et al. (1999) and Molénat et al. (2000) who studied groundwater flow and transport including discharge and rapid flow, compared it to simulated results and identified the governing flow and transport processes as well as the characteristic time of these hydrological systems. Based on these findings, we hypothesize that the spectrum of groundwater level fluctuations is predominantly determined by regional hydraulic properties of an aquifer and therefore can be used to reliably infer regional aquifer parameters to effectively parameterize a groundwater model at regional scales.

Our proof of concept builds on the following consecutive steps: First, we generate a 2D virtual aquifer setup and show that a spectrum can be used to reliably estimate aquifer parameters for an aquifer with a homogeneous hydraulic conductivity field. Then, we expand the homogeneous setup to various heterogeneous setups and demonstrate that the spectrum of the groundwater level fluctuations is predominantly determined by effective hydraulic properties of the aquifer and can be used to infer effective parameters. Third, we move from virtual 2D aquifers to real aquifers and compare spectra from real groundwater level time series with theoretical spectra. Moreover, real aquifer systems are three dimensional and groundwater flow lines and their lengths are not exactly known without a groundwater model but the length L is an essential prerequisite for our method. Therefore, we investigate the sensitivity of our method with respect to that length in a fourth step. Finally, we present a plausibility test of our method on four groundwater level time series of the Main catchment.

In the following theoretical part, the relevant groundwater flow equations and the spectral analysis method are described, followed by the numerical tools used. Then we provide the experimental setup to validate the first two steps of the proof of concept described above. We develop a method to infer regional aquifer parameters from a spectrum in a virtual aquifer setup. Subsequently, we show how spectra of real groundwater level time series can look like and how they compare to the theoretical considerations. It follows the sensitivity analysis of the developed method using real groundwater data and a plausibility test of the spectral approach. Finally, we summarize and discuss the field data analysis before we complete our work with a conclusion.

2. Theory

2.1. Equations of Groundwater Flow

Based on the conservation of water mass and Darcy's law, the flow of water through an anisotropic, saturated medium is described with the 3D groundwater equation (e.g., Freeze, 1979):

$$\frac{\partial}{\partial x}\left(K_x\frac{\partial h}{\partial x}\right)+\frac{\partial}{\partial y}\left(K_y\frac{\partial h}{\partial y}\right)+\frac{\partial}{\partial z}\left(K_z\frac{\partial h}{\partial z}\right)=S_s\frac{\partial h}{\partial t} \tag{1}$$

where S_s $[L^{-1}]$ and K $[LT^{-1}]$ are the specific storage and the hydraulic conductivity of the porous medium, respectively, and h $[L]$ states the groundwater level above an underlying aquitard. For an isotropic and homogeneous porous medium Equation 1 reduces to:

$$K\left(\frac{\partial^2 h}{\partial x^2}+\frac{\partial^2 h}{\partial y^2}+\frac{\partial^2 h}{\partial z^2}\right)=S_s\frac{\partial h}{\partial t} \tag{2}$$

In a shallow regional groundwater system with a horizontal extension much larger than its vertical, the vertical flow components are much smaller than the horizontal ones and usually neglected. Consequently, Equation 2 can be averaged across the vertical coordinate z. In a confined aquifer with constant thickness b $[L]$, the hydraulic conductivity and specific storage are then replaced by the transmissivity T $[L^2T^{-1}] = K$ $[LT^{-1}] \cdot b$ $[L]$ and the

storativity $S[-] = S_s\ [L^{-1}] \cdot b\ [L]$. If additionally groundwater recharge $W\ [LT^{-1}]$ enters the aquifer, Equation 2 finally becomes:

$$T\left(\frac{\partial^2 h}{\partial x^2} + \frac{\partial^2 h}{\partial y^2}\right) + W = S\frac{\partial h}{\partial t} \tag{3}$$

In unconfined aquifers the thickness does not depend on z but is given by the water level h which introduces a non-linearity in the flow (Equation 3). However, in shallow regional systems, water level variations are considered small against the overall water level and a constant thickness is presumed. Following this argumentation, Equation 3 describes both confined and unconfined shallow groundwater systems. The difference between them shows up in the storativity only. The storativity of confined aquifers is determined by the porosity, the compressibility of the aquifer, and the water itself and is usually very small. The storativity in unconfined aquifers comprises the compressibility of the aquifer, the water, and additionally, the specific yield $S_y\ [-]$. Since S_y is typically dominating the storage behavior of the aquifer, the storativity is effectively equal to S_y in unconfined groundwater systems.

Depending on the boundary conditions, groundwater might flow more or less uniformly along one spatial direction and Equation 3 can be even more simplified to

$$T\frac{\partial^2 h}{\partial x^2} + W = S\frac{\partial h}{\partial t} \tag{4}$$

where x axis is now aligned parallel to the groundwater flow direction. Assuming that the groundwater system is only supplied by groundwater recharge W from the top, groundwater might leave the system toward a river. The corresponding boundary and initial conditions describing such a groundwater system then read

$$h(x,0) = f(x); \quad \frac{\partial h}{\partial x}|_{x=0} = 0; \quad h(L,t) = h_0 \tag{5}$$

assuming an aquifer system of length L, a no-flow boundary condition at the water divide $x = 0$ and a fixed water level at the river boundary $x = L$ (Figure 2a).

Equation 4 together with its initial and boundary conditions (Equation 5) can be solved analytically. This still holds if the groundwater recharge is a temporally fluctuating function $W(t)$ and more complex boundary conditions are governing the groundwater flow behavior. Analytical solutions are presented in the articles by Liang and Zhang (2013), Liang and Zhang (2015), or de Rooij (2012).

2.2. Stochastic Temporal Behavior of Hydraulic Heads

A temporally fluctuating recharge $W(t)$ complicates the analytical solution and allows only to specify it as a convolution of $W(t)$ with basic expansion terms solving the homogeneous equation. However, considering $W(t)$ as a stochastic function in time with a known temporal mean $\overline{W}$, temporal variance σ_W^2 and auto-covariance function allows to solve Equation 4 stochastically. Making use of the calculus of stochastic differential equations, stochastic temporal moments can be evaluated as presented in the article by Liang and Zhang (2013). In their article, the authors argue that river fluctuations are in most cases relatively small compared to the groundwater level fluctuations in the aquifer so that their effects are limited to a small zone close to the constant-head boundary condition. Thus, they set T, S_y, and h_0 to be constant and consider only the recharge W as being stochastic in time following a white noise process. Our work focuses on the head spectrum S_{hh} (also: PSD, power spectrum, spectral density) which is the Fourier transform of the temporal auto-covariance function R_{hh} of groundwater levels. The solution will be discussed later in this subsection. First, the theoretical basis for the spectral approach is given.

The spectral approach is based on the Fourier transform, which transfers a signal $g(t)$ (e.g., measured groundwater levels over time) from the time to the frequency domain. The forward Fourier transform is defined as:

$$\hat{g}(\omega) = \int_{-\infty}^{\infty} g(t)\, e^{2\pi i \omega t}\, dt \tag{6}$$

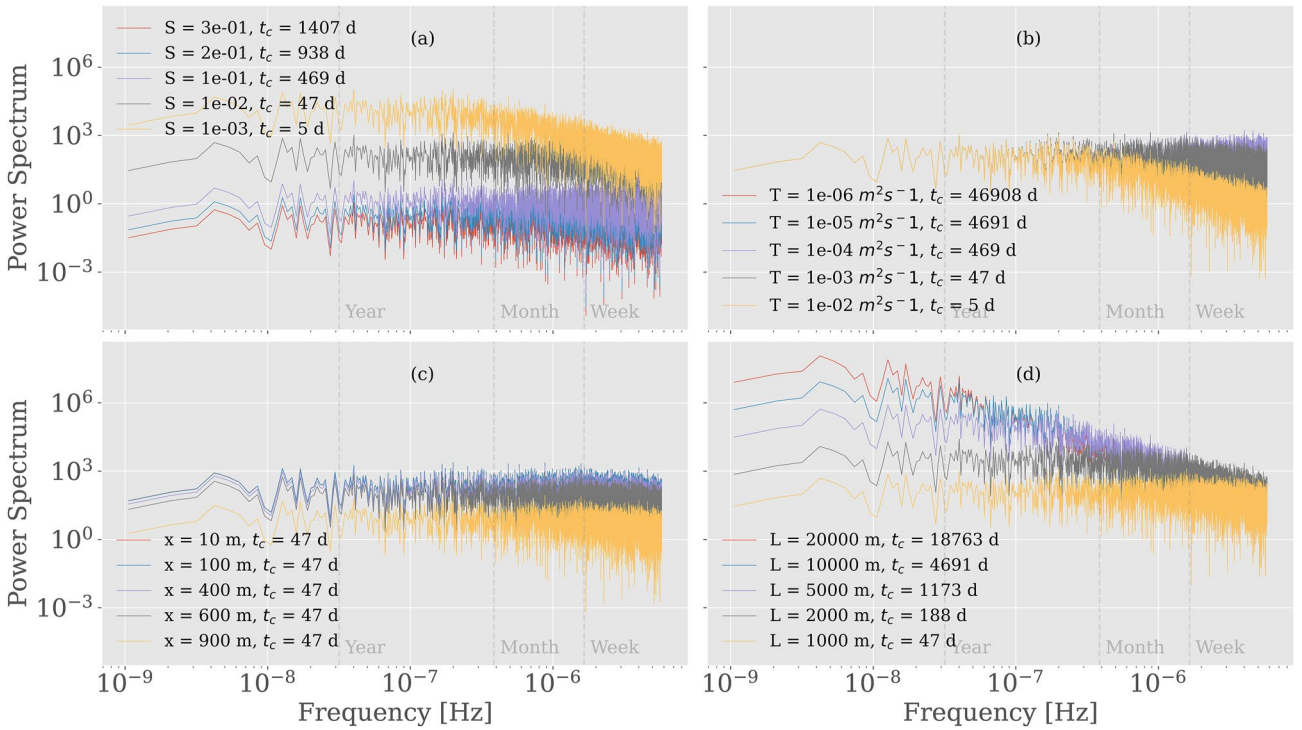

Figure 1. Semi-analytical power spectra of a hydraulic head fluctuation calculated with a white noise-like recharge. The recharge signal was sampled from a uniform distribution between the intervals 0 and 1 mmd^{-1} and has a constant power spectrum for frequencies larger than 0. In each subplot another parameter was varied: (a) storativity S (specific yield S_y in Equation 8); (b) transmissivity T; (c) position along the transect x; (d) aquifer length L. Except for varied parameters, remaining parameters are kept constant for each subplot: $S = 0.01$, $T = 0.001$ m^2 s^{-1}, $x = 500$ m, and $L = 1{,}000$ m. Vertical dashed lines mark frequencies which correspond to a period of 1 year, 1 month, and 1 week, from left to right, respectively.

where $i = \sqrt{-1}$ and ω is the frequency. The resulting signal $\hat{g}(\omega)$ represents the frequency share of the original signal, that is, it can be seen as the decomposition of the signal into sine waves of varying amplitude, phase, and period (Fleming et al., 2002).

Using the Fourier transform (Equation 6), Equation 4 can be transferred to the frequency domain, solved and S_{hh}—which is according to the *Wiener-Khinchin* theorem the Fourier transform of R_{hh} (Khintchine, 1934; Wiener, 1930)—can be evaluated.

$$S_{hh}(x,\omega) = \int_{-\infty}^{\infty} R_{hh}(x,\tau)\, e^{-2\pi i\omega\tau} d\tau \tag{7}$$

where R_{hh} is assumed to be stationary in time and τ is the time lag.

The head spectrum is given by

$$S_{hh}(x,\omega) = \frac{16}{\pi^2 S_y^2} \sum_{m=0}^{\infty}\sum_{n=0}^{\infty} \frac{(-1)^{m+n} B_m B_n S_{ww}}{(2m^2+2n^2+2m+2n+1)} \cdot \frac{(2m+1)^2}{(2m+1)^4 t_c^{-2} + \omega^2} \tag{8}$$

$$B_m = \frac{\cos\left[(2m+1)\pi x'/2\right]}{(2m+1)}, \quad x' = \frac{x}{L} \tag{9}$$

where t_c is the so called characteristic time of the aquifer (also referred to as characteristic time scale or aquifer response time), S_{ww} the spectrum of groundwater recharge fluctuations, x is the lateral position of the hydraulic head measurement, and L is the aquifer length from the water divide to the river. Assuming the recharge having a constant power spectrum (white noise-like) for frequencies larger than 0, the spectrum of hydraulic head fluctuations is shaped as displayed in Figure 1. A white noise is a process which is temporally uncorrelated and thus shows a spectrum which is constant for all frequencies. As mentioned in Section 1, the aquifer serves as a low-pass

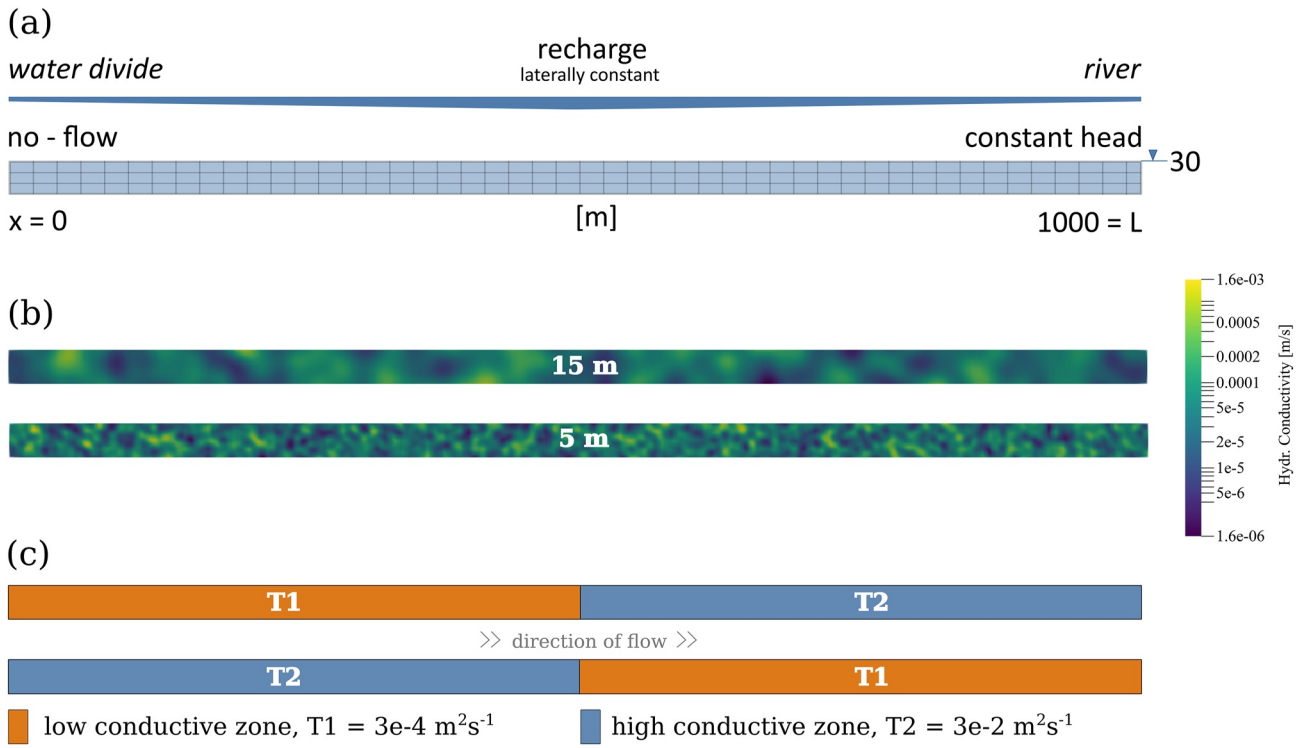

Figure 2. (a) Aquifer geometry, forcing and boundary conditions for all numerical setups. (b) One realization of each correlation length of an isotropic, log-normal distributed hydraulic conductivity field generated from a Gaussian covariance model with variance 1. Top: 15 m, bottom: 5 m correlation length. (c) Deterministic block aquifer with two zones of different transmissivity. The position of the boundary between the zones was varied throughout the different simulations.

filter which dampers higher frequencies and let pass lower frequencies of the signal almost unaltered. The onset of filtering is set by a specific frequency which is related to the inverse characteristic time (i.e., the hydraulic response time) of an aquifer which depends on the materials the water flows through. Increasing the storativity (Figure 1a), decreasing the transmissivity (Figure 1b), or extending the length of the aquifer (Figure 1d) results in larger characteristic times which implies that perturbations persist for longer times in the aquifer until they vanish. Larger characteristic times move the cut-off frequency to lower frequencies. In addition, the location of the groundwater level measurement x mainly influences the overall magnitude of the spectrum (Figure 1c).

Finally, we discuss the characteristic time t_c of an aquifer. In literature, many different definitions and different names are existing. Markovic and Koch (2014) call it characteristic aquifer time scale, van de Leur (1958) call it reservoir-coefficient, de Rooij (2013) just used the expression characteristic time, while Liang and Zhang (2013) did not use any specific terminology. The reason for these different names lies probably in the fact that different aspects in the temporal behavior of an aquifer are addressed. While surface hydrologists often mean by characteristic time the inverse recession constant (e.g., Gelhar, 1974) which describes the recession of baseflow when no recharge is feeding the aquifer, groundwater hydrologists usually relate it to the time until an aquifer reaches the near-steady state (e.g., 95% equilibrium) after a certain perturbation, t_{NE} (Carr & Simpson, 2018; Rousseau-Gueutin et al., 2013). However, all these definitions of a characteristic time have in common that it is proportional to $\frac{L^2 S_y}{T}$. The difference is only in changing the pre-factors.

Starting from Equation 4 and using the spectral approach, Liang and Zhang (2013) derive the characteristic time as

$$t_{Dup1} = \frac{4L^2 S_y}{\pi^2 T} \tag{10}$$

while others like Liang and Zhang (2015) (in a later paper), Wilkinson and Cooper (1993), and Jiménez-Martínez et al. (2013) or Russian et al. (2013) define it as

$$t_{Dup2} = \frac{L^2 S_y}{T} \tag{11}$$

skipping any pre-factor. Starting from Equation 4 but deriving a linear reservoir type model from it, Gelhar (1974) and Gelhar and Wilson (1974) define the characteristic time as

$$t_{Lin} = \frac{L^2 S_y}{3T} \tag{12}$$

Moreover, Molénat et al. (1999) and Molénat et al. (2000) state that the spectral response of a linear reservoir model and a Dupuit aquifer model can be equivalent for low frequencies when using a time scale as

$$t_c = \sqrt{6}\frac{L^2 S_y}{T} \tag{13}$$

Further definitions can be found in Manga (1999), Carr and Simpson (2018), and Erskine and Papaioannou (1997). In this work we define the characteristic time by (10) to be consistent with Liang and Zhang (2013).

The characteristic time can vary over orders of magnitude and depends strongly on the aquifer length. It might range from a few months for small and highly conductive aquifers with small specific storage to several years for large aquifers with small transmissivities and high storativities. For instance, if $L = 1000$ m, $S_y = 0.1$, $T = 0.01$ then $t_c = 47$ days and if $L = 5{,}000$ m, $S_y = 0.01$, $T = 0.001$ then $t_c = 1{,}172$ days. Figure S10 in Supporting Information S1 depicts the resulting characteristic times for different combinations of S, T, and L (aquifer length).

3. Numerical Tools

The groundwater simulations in this work were conducted with the open-source multi-physics software OpenGeoSys (OGS) version 5.7.1-49-g5255869 (Kolditz et al., 2012). OGS solves the 3D groundwater flow Equation 1 based on the finite element method and is widely used for modeling coupled thermo-hydro-mechanical-chemical processes in porous and fractured media. The source code is written in C++ and can be downloaded from the corresponding GitHub repository (https://github.com/ufz/ogs5) together with additional tools for pre- and post-processing including the OGS Data Explorer.

The research questions addressed in this paper made it necessary to work with large ensembles of numerical groundwater models. Setting up model domains including mesh generation, application of boundary conditions and groundwater recharge, and sampling aquifer parameters from large ensembles is tedious work. With *ogs5py* (Müller, 2019) API it is possible to generate OGS5 input files and run the current setup with python scripts. Furthermore, the output in form of VTK and TecPlot can be read and is directly available in python for further processing.

Heterogeneous stochastic hydraulic conductivity fields were generated and assigned to the grid cells with the combination of *ogs5py* and *gstools* (Müller & Schüler, 2019). The python package *gstools* (GeoStatTools) contains geostatistical tools for random field generation and variogram estimation. The complete geo-statistical framework can be accessed via https://geostat-framework.github.io/.

Simulated time series from the numerical models and observed time series from the field study were processed and their spectra were calculated making use of the *numpy* package. Time series data of groundwater levels at different locations in the domain are Fourier transformed using *numpy.fft*. The power spectrum was finally obtained by taking the magnitude squared of the Fourier transformation. The result corresponds to the Fourier transform of the auto-covariance function of the groundwater levels (Section 2.1). The resulting numerical spectra were evaluated at frequencies larger than 0 and fitted with least-squares optimization against the semi-analytical solution of the head spectrum from Liang and Zhang (2013) which depends on the transmissivity T, specific yield S_y, aquifer length L, and position x along the transect. The aquifer length and the position of the measurement location are prescribed and thus known and T and S_y are inversely determined from the fitted spectrum.

All python scripts for data processing and analysis as well as for the model establishment are available on GitHub and Zenodo (Houben, 2022) release version 1.0. The modeling results as well as the time series from the field

study are available in a collection on Zenodo (Houben, 2021). Additional information can be found in Supporting Information S1 or directly in the repository.

4. Design of Numerical Experiments

In this section, we describe the design of three sets of different numerical experiments which are based on simulations of groundwater flow through virtual aquifers. All virtual aquifers have the same geometry, the same boundary conditions at the upgradient water divide and at the downgradient river boundary, and the same groundwater recharge. They differ with respect to the selected hydraulic parameters.

The first set of simulations are conducted to prove the feasibility to infer the hydraulic parameters S and T from groundwater level spectra. Therefore, the virtual aquifer in this first experiment is chosen to be homogeneous. Real aquifers are, however, always heterogeneous and show heterogeneously distributed hydraulic parameters. Knowing the recharge and assuming that other hydrological processes play a minor role, we hypothesize that the spectrum of groundwater level fluctuations is mainly determined by large scale hydraulic properties. Therefore, the second set of numerical simulations builds on virtual aquifers with heterogeneously distributed hydraulic conductivity fields drawn from an isotropically distributed log-normal spatial distribution with a known effective hydraulic conductivity value, resulting in a known effective transmissivity value for a constant aquifer thickness. In addition to stochastic heterogeneity, often deterministic heterogeneity (i.e., zones of constant properties) are found in real aquifers. The third set of simulations therefore aims at investigating the impact of different zones on the estimation of representative hydraulic parameters of the aquifer breaking the ergodicity of the second setup.

In this work, we follow the terminology for representative hydraulic parameters as explained by Sanchez-Vila et al. (2006), where they consider a representative parameter to control the average behavior of groundwater flow at a given scale. They subdivide the terminology further as follows: effective parameters are obtained by averaging over an ensemble of realizations of a stochastic process which reveals a constant value for the entire domain under the assumption of ergodicity (setup 1 and 2). In case this value varies in space (i.e., in the presence of boundaries or source/sinks) it is termed as the pseudo-effective or apparent parameter. An equivalent parameter is obtained by averaging in physical space which is often referred to as block-averaged or volume-averaged, consequently upscaled parameter (setup 3). Finally, an interpreted parameter is defined in the physical space and obtained from the interpretation of field tests (e.g., pumping and slug tests, among others).

4.1. General Numerical Setup

The numerical model represents a rectangular aquifer system with a no-flow boundary condition at $x = 0$ (water divide) and a Dirichlet boundary condition (constant head) at $x = L$ (river) for the right boundary of the model domain (Figure 2), where L is the aquifer length from water divide to the river chosen to be 1,000 m. The river is fully penetrating, that is, connected over the entire thickness of 30 m. No-flow boundary conditions are implemented at the bottom of the model domain while groundwater recharge is added from the top (Neumann boundary condition). Groundwater recharge is constant in space but fluctuates temporally as a white noise-like signal sampled from a uniform distribution between the intervals 0 and 1 mmd^{-1} showing a constant power spectrum for frequencies larger than 0 and smaller than the Nyquist frequency ($f_{Nyquist} = 0.5 \cdot f_{sampling} = 0.5 \cdot (1/86{,}400\ \mathrm{s}) \approx 5.79^{-6}$ Hz).

For each model the modeling period spans 30 years (10,950 days) with a time step size of 1 day. The numerical models were set up with different spatial discretizations. In the first set of simulations (homogeneous setup, Section 4.2) the cell size was chosen to be 10×10 m, whereas in the other two sets (Section 4.3 and Section 4.4) a 1×1 m resolution was chosen. As initial condition for each transient simulation we set the steady state groundwater level distribution originating from a steady-state simulation with the temporal mean of the groundwater recharge.

4.2. First Setup: Homogeneous Virtual Aquifer

The aim of this experiment is to prove that T and S can be inversely estimated from groundwater level spectra.

Values for T and S were uniformly sampled (on a logarithmic scale) over a wide range of realistic values: the storativity values ranged from $1 \cdot 10^{-5}$ to $1 \cdot 10^{-1}$ [−] and transmissivity from $1 \cdot 10^{-6}$ to $1 \cdot 10^{-2}$ m^2 s^{-1}. Each parameter was sampled 41 times resulting in a total number of 1,681 independent models. The relative deviation between the true model parameters, transmissivity (T) and storativity (S), and the inversely estimated parameters of the spectral analysis at several locations in the aquifer was evaluated using the formula $Error[\%] = \frac{|Input - Output|}{Input} \cdot 100$.

4.3. Second Setup: Virtual Aquifer With Stochastic Heterogeneity

In order to investigate the spectral response of a heterogeneous aquifer system, we generated random, isotropic, and log-normal distributed hydraulic conductivity fields. The geometric mean was set to approximately $4.5 \cdot 10^{-5}$ m s^{-1}. The isotropic spatial correlation structure was determined by a Gaussian covariance function with variance 1 and two different correlation lengths of 5 and 15 m (Figure 2). For each stochastic hydraulic conductivity field, 200 realizations were generated. The specific storage in this experiment was set to $1 \cdot 10^{-3}$ [−] and was constant for all simulations.

4.4. Third Setup: Virtual Aquifer With Deterministic Heterogeneity

In the third numerical experiment, we simulated aquifer transects with two distinct zones of transmissivity (Figure 2c).

In the first model from setup (c) (Figure 2c) the lower conductive zone was placed in the upgradient part of the aquifer and the higher conductive part downgradient, whereas in the second model the arrangement was swapped. Moreover, we kept the specific storage constant ($S_s = 10^{-4}$). The aquifer thickness was constant in the whole domain, and thus the transmissivity results from multiplying the hydraulic conductivity with the thickness of 30 m. The transmissivity of the low conductive zone was set to $T1 = 3 \cdot 10^{-4}$ m^2 s^{-1} and that of the high conductive zone to $T2 = 3 \cdot 10^{-2}$ m^2 s^{-1}. The interface between these two zones was moved step wise from $x = 10$ to $x = 990$ m with increments of approximately 50 m. For simplicity, we show in this paper the results of three locations only: the two extreme locations ($x = 10$ and 990 m) and one intermediate setting ($x = 500$ m). Additional settings can be found in Supporting Information S1.

5. Numerical Experiments: Results and Discussion

5.1. First Setup: Homogeneous Virtual Aquifer

In Figure 3 we summarize the results of this experiment and plot the relative error of the estimated parameters T and S against the characteristic time t_c.

For a modeling period of 30 years and a time step size of 1 day we can make the following statements: the estimated values for T and S matched the real parameter values for a wide range of t_c almost precisely with differences between T and S for specific ranges of t_c. T could be estimated for aquifers with a t_c ranging from 0.1 days to approximately 1,000 days within an error of 5% (Figure 3b). Only in aquifer systems with characteristic times larger than approximately 1,000 days, the estimation of T was prone to errors. Moreover, the estimated values did not strongly depend on the spatial location where the spectrum has been evaluated.

For the storativity, the error was large for aquifer systems with characteristic times smaller than a day (Figure 3), whereas we found an accurate estimation for aquifer systems with a t_c between 1 and approximately 1,000 days. For characteristic times t_c larger than 1,000 days, the error increased again and showed in addition a stronger dependence on the spatial location in the aquifer. Closer to the river, the error was largest and exceeds values of more than 60%. Closer to the no-flow boundary condition (water divide) the error was much smaller.

In order to explain our results we need to recall two aspects: First, any real time series has a finite total length and a finite temporal discretization which results in an upper and a lower bound for frequencies which can be contained in the signal. In our case, the upper bound was determined by time discretization of 1 day leading to an upper frequency of about 1/day whereas the total length of the time record of 30 years set the lower bound. Second, having a closer look at Equation 8, we see that the spectrum is characterized by two regimes: a frequency regime with frequencies smaller than the inverse characteristic time t_c and one with frequencies larger than $1/t_c$. In the regime $\omega < 1/t_c$, the spectrum depends on T but not on S, which is consistent with the fact that small

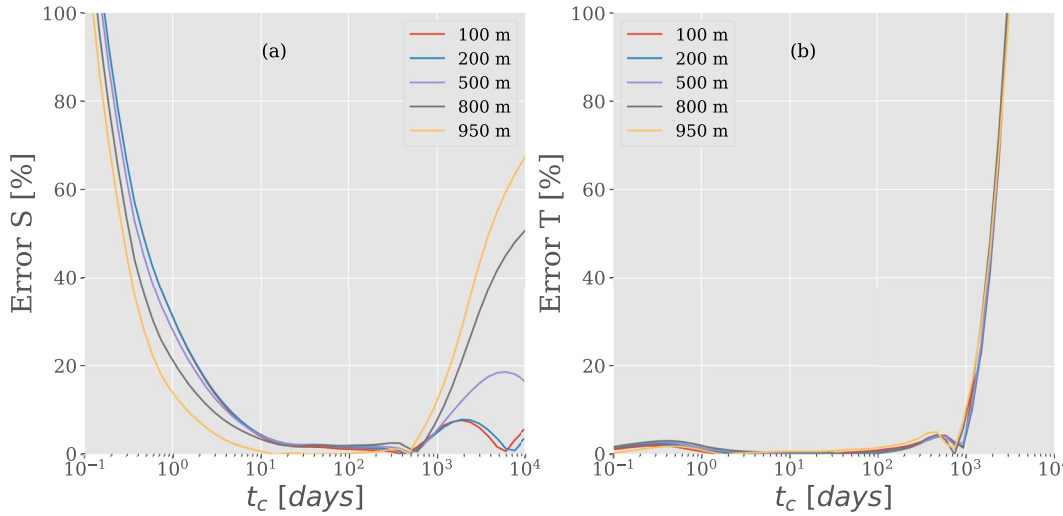

Figure 3. Error of deviation between input (numerical model) and output (spectral analysis) aquifer parameters with respect to input parameters plotted against the characteristic time t_c of the aquifer for five locations. The error was evaluated using the formula $Error[\%] = \frac{|Input - Output|}{Input} \cdot 100$. (a) Error of storativity and (b) error of transmissivity.

frequencies are equivalent to long times and the steady state of the hydraulic head distribution depends only on T. For $\omega > 1/t_c$, high frequencies representing the short time behavior and with that S is dominating the temporal behavior of the aquifer.

Combining these two aspects, it is evident that in very slowly responding aquifers with characteristic times t_c of about 30 years $\approx 10^4$ days, no T can be estimated if the time series just comprises 30 years in total. Consequently, if time series records are limited, the spectral analysis should be applied in shorter and higher conductive aquifers with small storativities in order to ensure correct estimates of the power spectrum and therefore correct estimates of T. In the other extreme of very quickly responding aquifer systems with characteristic times of about a day, no S can be estimated by making use of groundwater levels measured with just daily resolution. Some examples of head power spectra and their fit with the semi-analytical solution can be found in Supporting Information S1. Furthermore, Figure S10 in Supporting Information S1 depicts the resulting characteristic times based on Equation 10 for different combinations of S, T, and L. We included the obtained results concerning the minimum length of the time series, so that it can be easily seen which aquifers required certain lengths of groundwater records.

In addition to these constraints, a look at formula 8 shows that an estimate close to the river is hampered since the cosine function in the spectrum is approaching zero.

All our simulation results are consistent with these considerations and support our hypothesis that a thin, confined 2D groundwater system can be approximated by the 1D analytical solution of the linearized Boussinesq equation of Liang and Zhang (2013) with the following restrictions to the length of the simulation time and the temporal discretization: (a) The simulation time should cover at least a period which is approximately 10 times as long as the characteristic time of the investigated aquifer system to obtain a correct estimate of the spectra, thus correct estimates of T, and (b) the temporal discretization should be at least slightly smaller than the characteristic time to model the full transient behavior correctly. Respecting these conditions, it is possible to robustly estimate S and T from groundwater level spectra.

5.2. Second Setup: Stochastic Virtual Aquifer

In the second experiment, hydraulic head time series of two stochastic ensembles (differing by the spatial correlation length) and at different locations (100, 200, 500, 800, 940 m) were analyzed. The kernel density estimates of the inversely estimated aquifer parameters are depicted in Figure 4 against the different locations. Red and blue illustrate the distribution of estimated T and S values for the two different ensembles of 5 and 15 m correlation length, respectively. The storativity and the geometric mean of the transmissivity were held constant throughout all realizations.

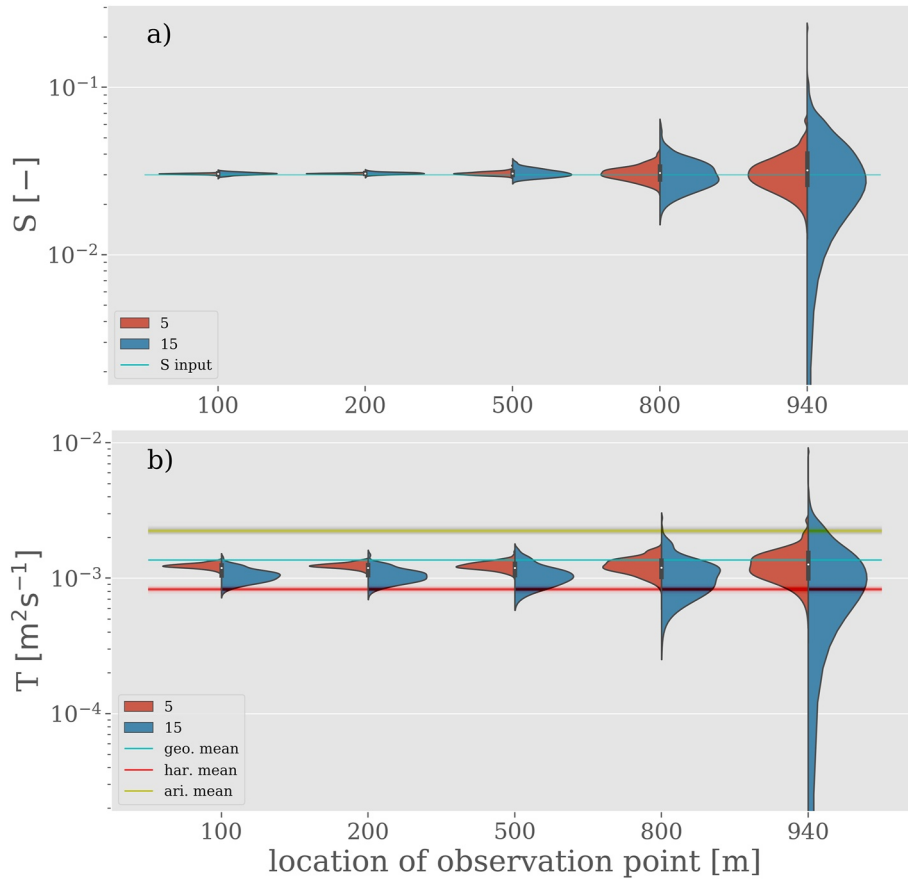

Figure 4. Kernel density estimate for determined aquifer properties by spectral analysis of hydraulic heads for 200 realizations of a stochastic (log-normal distributed K-field) aquifer, evaluated at different locations. Red and blue indicate 5 m and 15 m correlation length, respectively. The characteristic time t_c considering the geometric mean and Equation 10 is 108 days. (a) Derived storativities. The input storativity of the numerical model was held constant throughout all realizations ($S = 0.03$). (b) Derived transmissivities. The arithmetic, geometric, and harmonic mean of the underlying distribution are depicted with horizontal lines.

Figure 4a summarizes the inversely estimated storativity values. For locations close to the no-flow boundary condition and at the center of the aquifer ($x = 100, 200, 500$ m) the spread of the estimated parameter distribution was very small. In particular, the storativity could be estimated for both correlations lengths with high accuracy and precision. For observation points closer to the river ($x = 800$ m) the distribution started to spread, and the spread was highest at location $x = 940$ m since the ergodicity of heterogeneity was no longer satisfied. Nevertheless, the center of the distribution fell exactly on the correct storativity at all locations and for both correlations lengths.

Evaluating the transmissivity in Figure 4b, we observe a similar pattern like for the storativity: the precision of the estimates of the transmissivity was higher when approaching the water divide. In general, the center of the distributions fell slightly below the expected value (the geometric mean, also: the effective hydraulic conductivity) of the heterogeneous transmissivity field at all positions and both correlation lengths. The deviation from the geometric mean was higher for the ensemble with correlation length of 15 m, which was expected. According to the literature, the effective hydraulic conductivity approaches the geometric mean for two dimensional flow (e.g., Bakr et al., 1978; Dagan, 1979; de Marsily et al., 2005; Desbarats & Srivastava, 1991; Gutjahr et al., 1978) and log-normally distributed hydraulic conductivity fields. Higher correlation lengths lead to larger parts of less variable hydraulic conductivity, thus reducing the flow problem continuously from 2D to 1D if the correlation length approaches (half) the domain thickness (e.g., Pechstein & Copty, 2021; Schneider & Attinger, 2008). For 1D flow the effective hydraulic conductivity was expected to be equal to the harmonic mean (Bear, 1972; Gutjahr et al., 1978; Smith & Freeze, 1979). This explains why effective transmissivity values smaller than the geometric

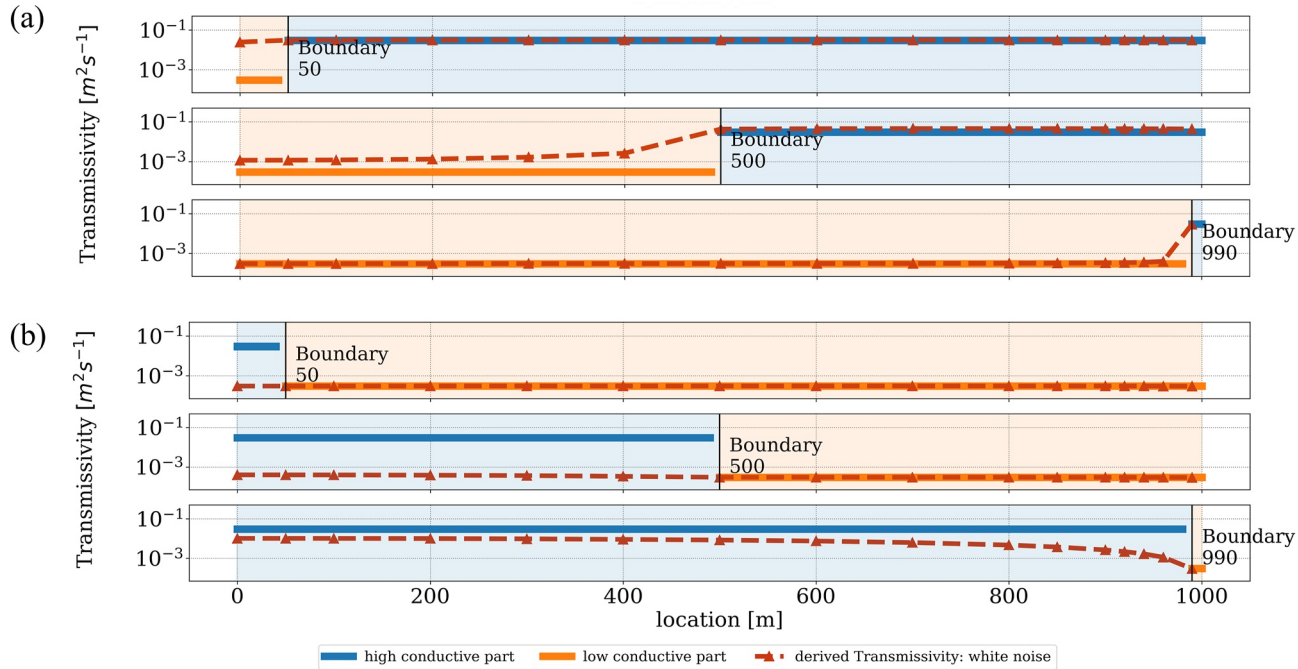

Figure 5. Input (numerical model) and output (spectral analysis) transmissivity for six different deterministic aquifers. A white noise-like recharge was assigned to the numerical model. (a) A low conductive zone in the upgradient part of the aquifer and a high conductive zone at the outlet. (b) A high conductive part upgradient and a low conductive part downgradient. Characteristic times of the low and high conductive zones considering Equation 10 are approximately 47 and 0.47 days, respectively.

mean were deduced in this experiment. In order to obtain values which precisely match the geometric mean, a smaller correlation length (at least along z) should have been chosen.

In general, our results support the hypothesis that the spectrum of groundwater level fluctuations is mainly influenced by effective and larger scale hydraulic properties when the recharge is known and effects from other hydrological processes (river stage, topography, tides, etc.) can be neglected. With that, spectral analysis has proven to be a valuable method to infer regional hydraulic parameters from local groundwater measurements.

5.3. Third Setup: Deterministic Block Aquifer

The results of the spectral analysis for six block aquifers are depicted in Figure 5. The solid lines represent the input parameters of the numerical model for the respective block. The spectral analysis was performed at different locations in the aquifer (see horizontal positions of markers) and the determined transmissivities are represented with a dashed red line for a white noise-like recharge. A plot of the recharge is included in Supporting Information S1.

In scenario (a), the water flowed from the low conductive to the high conductive zone. Low and high conductive zones could be correctly estimated but with a smooth transition zone of about 100–200 m between them instead of the sharp physical transition existing in reality. Moreover, the downgradient high conductive zone seems to have an impact on the inversely estimated low conductive zone located upgradient by stating too high transmissivity values. The extend of the low conductive zone upgradient in (a1) and (a2) is still too small in order to significantly reduce the equivalent transmissivity obtained from spectral analysis.

In scenario (b) the setting was swapped. The high conductive zone T_{high} was located in the upgradient part and the low conductive zone T_{low} in the downgradient part. The low conductive zone was well identified with its correct value T_{low}. The low conductive zone, however, tremendously also impacted the parameter inversion in the high conductive zone upgradient leading to transmissivity values which were considerably lower than the actual model input parameter. This supports the hypothesis that the variations in groundwater level at a given point may contain information about the hydraulic properties of the adjacent zones and, therefore, regional information related to equivalent (averaged) hydraulic parameters. Consequently, we were able to identify the low permeability zone at

the outlet while sampling groundwater in the adjacent and higher conductive materials. Moreover, the transition zone between the two estimated zones was tremendously increased compared to scenario (a): a larger low conductive zone leads to a larger transition zone. Even a very small low conductive zone at the outlet of the aquifer (Figure 5b, bottom) influenced the regional aquifer response of that zone. This fact is already known and can be easily calculated with the harmonic mean of Darcy's equation, yet with spectral analysis it is possible to illustrate this effect clearly. Consequently, accumulating materials at the river which cause a clogging of the flow might lead to entirely different equivalent hydraulic parameters than would be expected just from the material properties of the aquifer itself, making the spectral analysis potentially a more appropriate tool for estimating the regional hydrologic system than classical hydraulic tests. Figures S5 and S6 in Supporting Information S1 depict several models with other intermediate boundary settings.

Also the third set of experiments impressively demonstrated that the spectral analyses of sufficiently long time series can be a feasible tool to derive regional aquifer parameters.

6. Field Data Analysis

In the first part of the paper we analyzed two dimensional virtual homogeneous, stochastic and deterministic block aquifer systems and our results indicated a general feasibility of the spectral approach to estimate regional aquifer parameters. In this section, we move toward real aquifers with measured groundwater data and will shortly explain the additional challenge we face: our approach needs the aquifer length L, that is, the groundwater flow line and the position x where the groundwater observation well is located. Groundwater flow lines start at a water divide and end a river system. Unfortunately, finding and tracking groundwater flow lines is not a trivial task in three dimensional complex shaped aquifer systems. The lengths L differ within the catchment and also the positions of the head measurements need to be described with respect to their flow lines. Consequently, L and x are subject to large uncertainty. Therefore, we perform a sensitivity analysis to quantify how sensitive knowledge of L and x is to the application of our method.

Before the results of the sensitivity analysis are presented, we provide a general hydrogeological overview of the selected catchment and discuss groundwater level spectra of the four investigated observation wells. We close this section with a plausibility test of the spectral analysis using the measured groundwater level time series.

6.1. Hydrogeological Overview

Four observation wells in the Main catchment in central Germany were chosen in order to inspect the shape of their spectra. The catchment covers an area of 27,292 km^2. In this study we focused on the northern part of a subordinate catchment located in the south of the Main catchment (Figure 6). The northern part covers an area of approximately 940 km^2. Erosion has shaped the landscape remarkably cutting valleys into the sandstone and creating elevations of 400–440 m.a.s.l. on the high plateaus to depressions of 240 m.a.s.l. close to the Regnitz river. The dominant aquifer in this region, especially in the western part, is the *Burg- und Blasensandstein* which drains toward the Regnitz, a tributary of the Main river and is stratigraphically assigned to the middle Keuper as triassic sediments (Henningsen & Katzung, 2011).

We selected two groundwater observation wells (*Birkach*, *Strullendorf Nord*) screened in the dominant aquifer (*Burg- und Blasensandstein*) and two shallow observation wells installed in the Quaternary sediments from the valley fillings (*Stegaurach*, *Strullendorf West*). These wells were chosen since the groundwater records cover a sufficiently long time period, they are classified as shallow observation wells (except for Strullendorf Nord) and the aquifer is relatively homogeneous and conductive. Details about the heterogeneity of local subsurface flow conditions are unknown but following the interpolated groundwater levels, statements about the general drainage direction could be made, which informed the placement of the transect and finally helped to estimate the aquifer length, that is, the length from a water divide to the river. The groundwater data is freely available under license CC BY 4.0 and was downloaded from the online service of the Bavarian State Office for the Environment (https://www.gkd.bayern.de/de/grundwasser/oberesstockwerk). A section of the groundwater level time series of the observation wells are depicted in Figure 7. The records from *Strullendorf West* comprise the longest time period starting in the early 1970s. The time series from the observation well *Stegaurach* covers roughly 33 years starting in 1986, whereas the records from well *Strullendorf Nord* and *Birkach* start in 1998 and 2000, respectively, covering the shortest period. In the early years of the monitoring period the measurements were taken irregularly

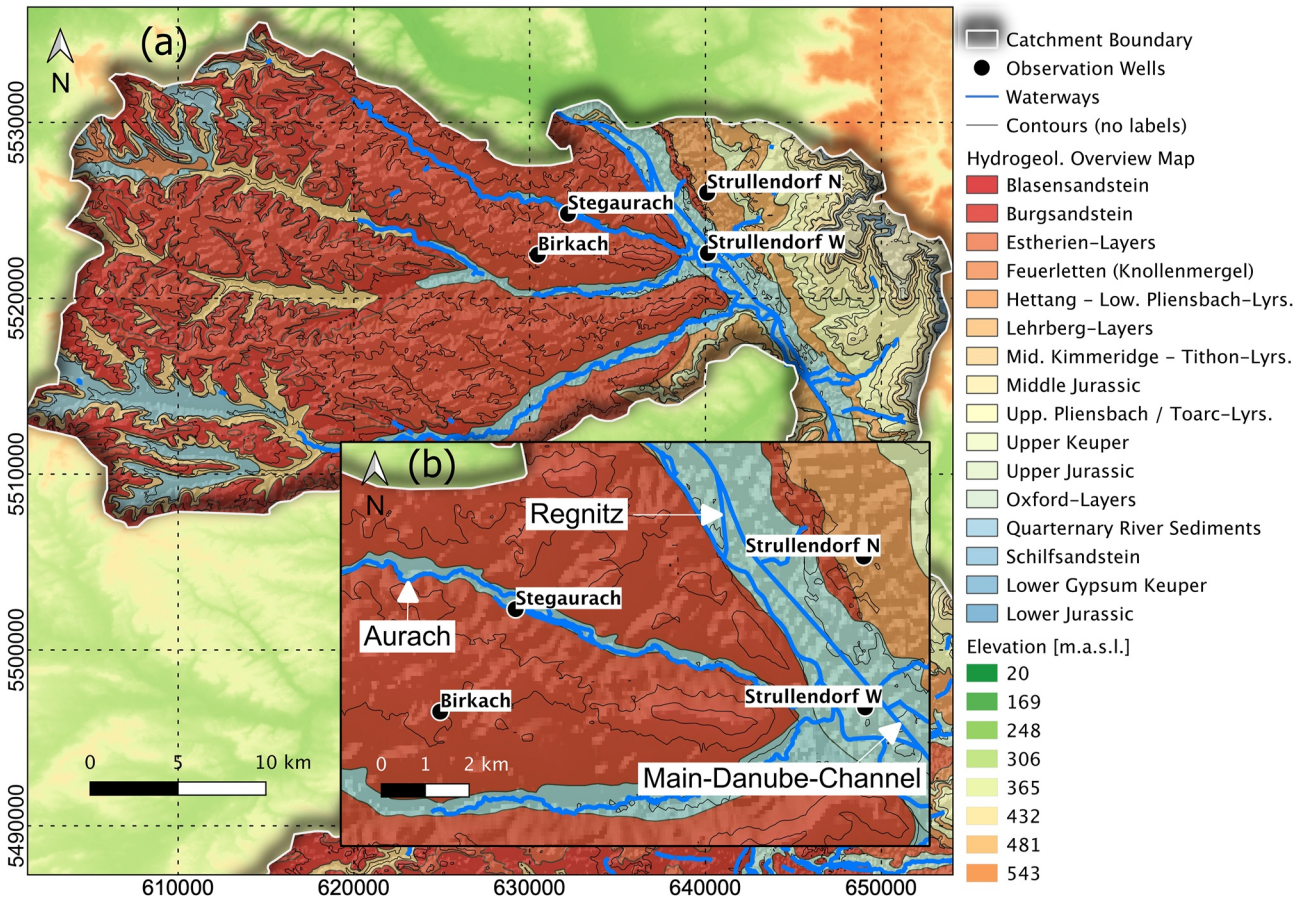

Figure 6. (a) Subordinate catchment in the south of the Main catchment in central Germany. Topography is indicated with black lines (no labels) and the geology with colored layers. The CRS is ETRS89/UTM zone 32N (EPSG:25832). (b) Zoom closer to the four investigated groundwater observation wells and the valley with the Regnitz river. The waterways were downloaded from OpenSteetMap (http://download.geofabrik.de), the SRTM was provided by the German Research Center for Air and Space Travel (DLR, https://eoweb.dlr.de/egp/), and the hydrogeological overview map (HUEK200) was published by the Federal Institute for Geosciences and Natural Resources (BGR, https://produktcenter.bgr.de/terraCatalog/Start.do).

and with different time intervals. Using the spectral approach requires a time series with constant time steps. This was accomplished by gap filling via quadratic interpolation.

In addition to hydraulic head data, the spectral analysis also requires groundwater recharge time series. Since groundwater recharge is difficult to measure, we use modeled recharge data provided by the hydrological model mHM (Kumar et al., 2013; Samaniego et al., 2010; Zink et al., 2017), which ran at a spatial resolution of 4×4 km for the Main catchment. The recharge time series are plotted in Figure 7 with bar plots of different colors corresponding to the respective location. The time series show similar temporal patterns at all observation wells. In contrast to that, the fluctuations of the groundwater levels systematically differ at the different locations: groundwater levels at *Stegaurach* as well as *Strullendorf West* react quickly to strong recharge events (e.g., in summer 2013) and show a short response time duration. In contrast to these shallow aquifer systems, the groundwater levels in the deeper aquifers (*Birkach*, *Strullendorf Nord*) respond slower to recharge events and show longer relaxation time periods up to 2 years.

6.2. Spectra of Groundwater Recharge and Groundwater Levels—General Insights

Groundwater recharge and head spectra were calculated and depicted in Figure 8. All groundwater recharge spectra have a similar form decreasing with $\omega^{(-\nu)}$ for times larger than a year corresponding to frequencies smaller than 1/year matching the theoretical shape of the spectrum based on Equation 8 very well for larger frequencies. The exponent ν is constant for times between a year and a month and larger than that for time scales smaller than

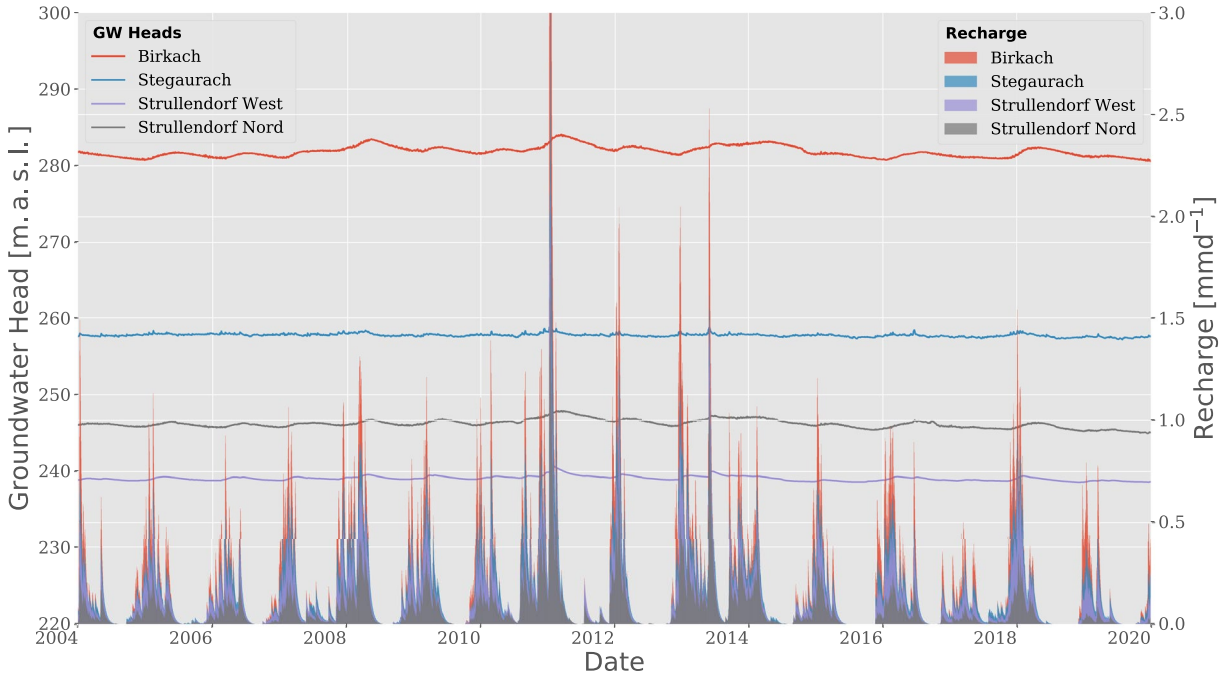

Figure 7. Groundwater level time series of four observation wells in the central Main catchment and corresponding recharge modeled with mHM.

months and weeks. This behavior may indicate that different processes govern the yearly and sub-yearly recharge behavior.

Despite this analogy, the groundwater level spectra vary between locations in shallow and deeper aquifer systems. The spectra in the deeper formations *Birkach* and *Strullendorf Nord* decrease with a higher exponent than *Stegaurach* and *Strullendorf West* (Figure 7) for times between a year and a month and show no filtering behavior for

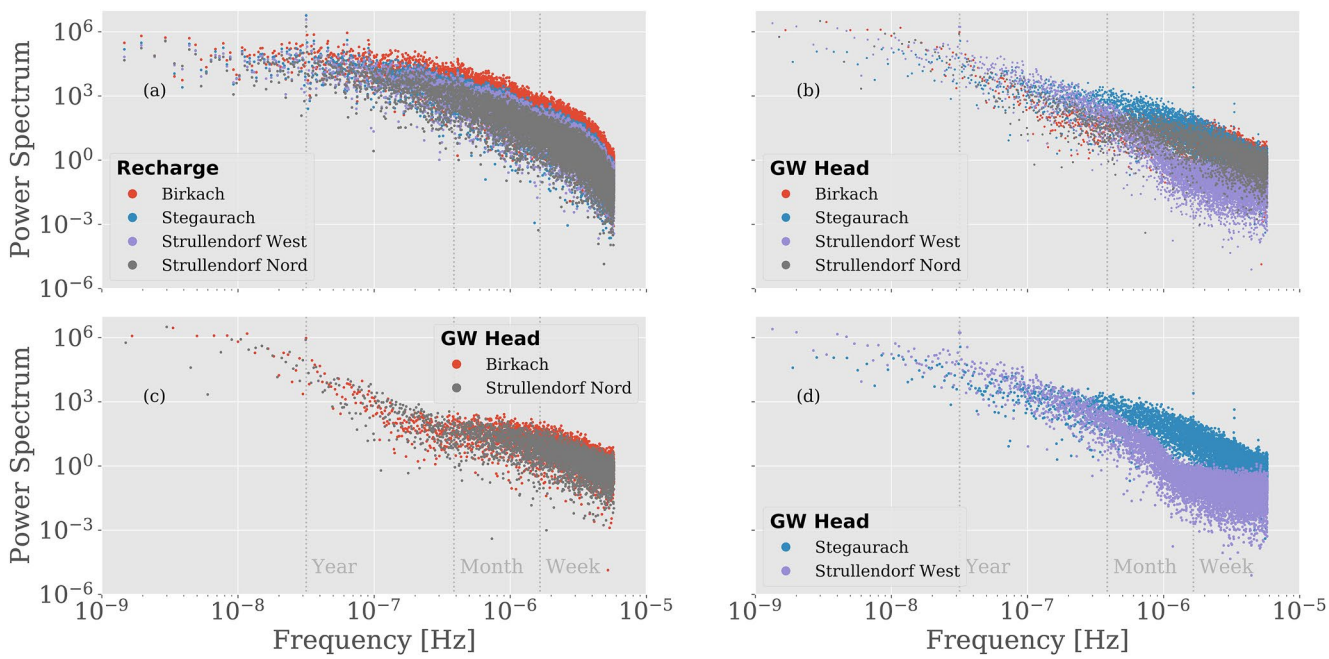

Figure 8. Power spectra of recharge (a) and groundwater level time series (b) for each observation well. For a better view, geologically similar wells are plotted in one figure: (c) screened in *Burg- und Blasensandstein* and (d) screened in quaternary sediments.

time scales between a month and a week. In contrast, the shallow systems *Stegaurach* and *Strullendorf West* still show filtering behavior for time scales between a month and a week.

Figure 8c depicts the spectra from observation wells *Birkach* and *Strullendorf Nord* which both are screened in the *Burg -und Blasensandstein* thus representing a deeper groundwater system. Although the locations *Birkach* and *Strullendorf Nord* have a distance of roughly 10 km from each other and are situated on opposite sites of the Regnitz river (Figure 6) they still show a similar spectral response, giving evidence that the spectra mainly describe the regional aquifer behavior than the local one.

The observation wells *Stegaurach* and *Strullendorf West* in Figure 8d represent a shallow groundwater system which is highly sensitive to recharge perturbations and river stage fluctuations. *Stegaurach* shows a similar spectrum like the one of the corresponding mHM based groundwater recharge. The similarity to the recharge gives evidence that the estimated recharge from the mHM model was predicted quite accurately and the filtering property of the aquifer is weaker compared to *Birkach* and *Strullendorf Nord*. The spectrum shows only little influence of lateral inflow. In contrast to this, the spectrum of *Strullendorf West* is impacted by additional forcings, presumably the fluctuations from the river *Regnitz*.

6.3. Sensitivity Analysis

After considering general features of the groundwater spectra of the four observation wells we now focus on the sensitivity analysis.

Before we start the analysis, we recall the formula of the spectrum (8). In the simple one dimensional aquifer, the spectrum only depends on three different sets of parameters: S, T/L^2, and x/L which implies that only the ratio x/L and T/L^2 can be inferred from the spectrum but not T separately. In the virtual aquifer system, the length of the aquifer was known, in real aquifers we do not know it beforehand. Only if we have geological expertise together with some knowledge of the flow system, the aquifer length L can be roughly estimated. Therefore, we test the sensitivity of L and x/L on the inversion of T and S.

For that purpose we randomly sampled x and L from a log-normal distribution with reasonable limits. We grouped them imposing the constrain $x < L$ and created a sample size of 243 samples. The goodness of fit was evaluated by R^2. The resulting values for T, S, and t_c as well as the evaluation metric for the goodness of the fit R^2 are depicted in the scatter plots in Figure 9.

We start with a discussion of the sensitivity results for the different parameters S, T, and t_c and continue in the following subsection by providing a range of the aquifer length L for each observation well which was estimated with hydrogeological expertise.

The first column on the left of Figure 9 shows the estimated storativity S. The variations in the estimated S are very small over all samples and all observation wells. Only for samples where L is approximately equal to x (close to the river) a decrease is noted, that is, the sensitivity increases when x approaches L. In addition, using field data and maps, it is usually straightforward to determine whether the observation well is very close to a river in relation to the aquifer length or whether it is situated in the aquifer body. Consequently, S can be robustly estimated even without knowing the exact values for L and x, especially when the observation well is not too close to the river. The same holds for the characteristic time (third column from the left): t_c is determined through S and T/L^2. The results show that both can be estimated robustly leading to good estimates for the characteristic time. In contrast, the estimation of T (second column from the left) is more uncertain which is explained by the fact that L is not known precisely. However, if L and x are known within an uncertainty below approximately one order of magnitude, which is realistic in real groundwater systems, the transmissivity can still be estimated quite precisely with an uncertainty of less than one order of magnitude. All these findings are consistent with results of the parameter inversion in the virtual aquifer system and impressively confirms the feasibility of the spectral method.

6.4. Plausibility Test

We close this section with a plausibility test. One possibility to achieve a reasonable estimate of the aquifer length is to follow the steepest groundwater gradient (groundwater flow direction) from the observation well toward the stream as well as in opposite direction, from the well toward a local groundwater maximum (e.g., a summit) and

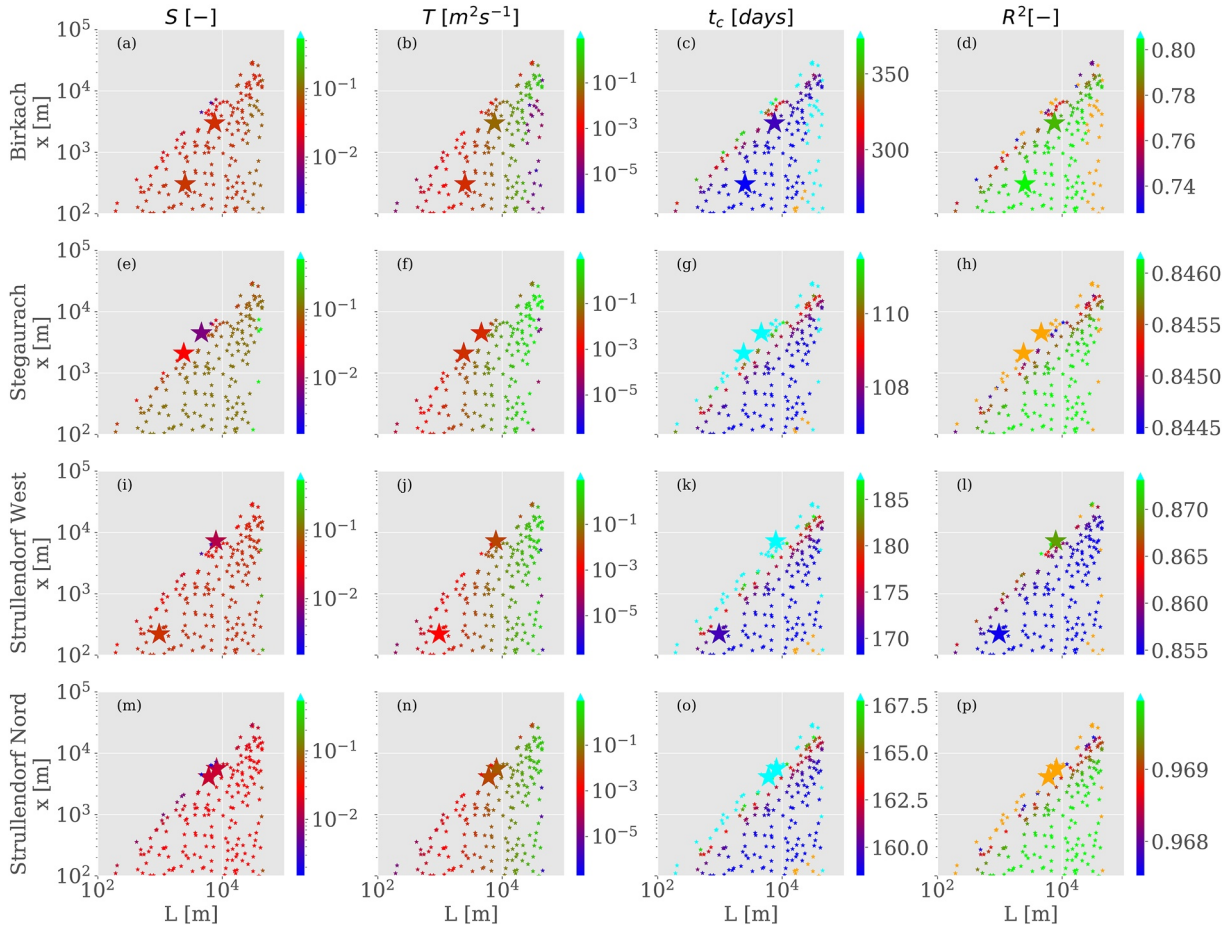

Figure 9. Scatter plots of derived storativity S, transmissivity T, and resulting characteristic time t_c for different combinations of aquifer length L and distance to water divide x. The goodness of the fit was evaluated with the R^2 value. Color bars of S and T have the same log-scale for every observation point with a value range according to the 5%–95% quantile range. The linear scale for t_c and R^2 was adjusted in each plot according to the 15%–85% quantile range. Values which are higher or lower than the color bar range are depicted in cyan and orange, respectively. The big stars represent the value range estimated with geological expertise which are discussed in Section 6.4. Histograms of every scatter plot can be found in the supporting information.

assume the sum of these two paths to be the aquifer length L. The position of the measurements x is then equal to the length of the upgradient segment. To preserve the assumptions of the semi-analytical model, we ensured that the upgradient and downgradient segments are parallel, that is, form a straight line from the summit toward the river intersecting the groundwater observation well. Within the ranges of hydrogeological interpretation of the orientation of the flow regime supported by the analysis of groundwater level maps, geological profile (data source: Bavarian State Office for the Environment, www.lfu.bayern.de), hydrogeological maps including digital elevation models as well as hydrological catchment delineations, we identified a maximum and minimum aquifer length. The parameters were inserted into Equation 8 and S, T, and t_c were inversely estimated. The results are listed in Table 1 and the head spectra including the least squares fit of the semi-analytical solution are depicted in Figure 10. The resulting transects are depicted in Figure S9 in Supporting Information S1.

The estimation of the aquifer length L and the position x for *Birkach* have a high uncertainty. The range for L was detected to be between 2,528 and 7,509 m. Therefore, the possible range for the transmissivity covers almost one order of magnitude (Table 1). By evaluating the R^2 (Figure 9) values we can clearly identify a better fit for positions of the observation well in the body of the aquifer which limits the possible range of lengths L. t_c is then estimated to be between 259 to approximately 273 days.

Stegaurach is situated close to the river. Therefore, the selected aquifer length and position x are almost identical. It resulted in robust estimates for all three parameters T, S, and t_c. Surprisingly, the R^2 value is lowest for samples where L almost equals x. Although the well was screened in quaternary sediments, it might be

Table 1
Results of the Spectral Analysis for the Manually Estimated Range of Aquifer Length L and Position of Groundwater Measurement x Based on Geological Expertise

		S [−]	T [m^2 s^{-1}]	t_c [days]	L [m]	x [m]
Birkach	max L	$4.86 \cdot 10^{-2}$	$4.71 \cdot 10^{-2}$	273	7,509	2,997
	min L	$5.41 \cdot 10^{-2}$	$6.26 \cdot 10^{-3}$	259	2,528	304
Stegaurach	max L	$6.41 \cdot 10^{-3}$	$5.39 \cdot 10^{-3}$	119	4,619	4,500
	min L	$2.97 \cdot 10^{-2}$	$6.93 \cdot 10^{-3}$	116	2,408	2,100
Strullendorf West	max L	$1.21 \cdot 10^{-2}$	$1.37 \cdot 10^{-2}$	258	7,910	7,250
	min L	$5.15 \cdot 10^{-2}$	$1.33 \cdot 10^{-3}$	171	968	220
Strullendorf Nord	max L	$1.52 \cdot 10^{-2}$	$2.71 \cdot 10^{-2}$	173	8,100	5,600
	min L	$1.56 \cdot 10^{-2}$	$1.55 \cdot 10^{-2}$	172	6,032	4,100

possible that the water which passes the observation well drains toward the next bigger river, the Regnitz. This hypothesis is supported by the shape of the spectrum (Figure 10b) which shows an almost constant slope (Schilling & Zhang, 2011) but also some additional perturbations which flatten the curve and might stem from river fluctuations.

Strullendorf West is located in the valley very close to the Regnitz river which fits to the result that the R^2 values were highest when L almost equals x. The aquifer length was not easily identifiable and varied between 968 and 7,910 m. Consequently, T varies over one order of magnitude. The general shape of the spectrum follows the theoretical Dupuit-aquifer (considering the mHM recharge) for a wide frequency range (Figure 10c) which lead to a good overall fit.

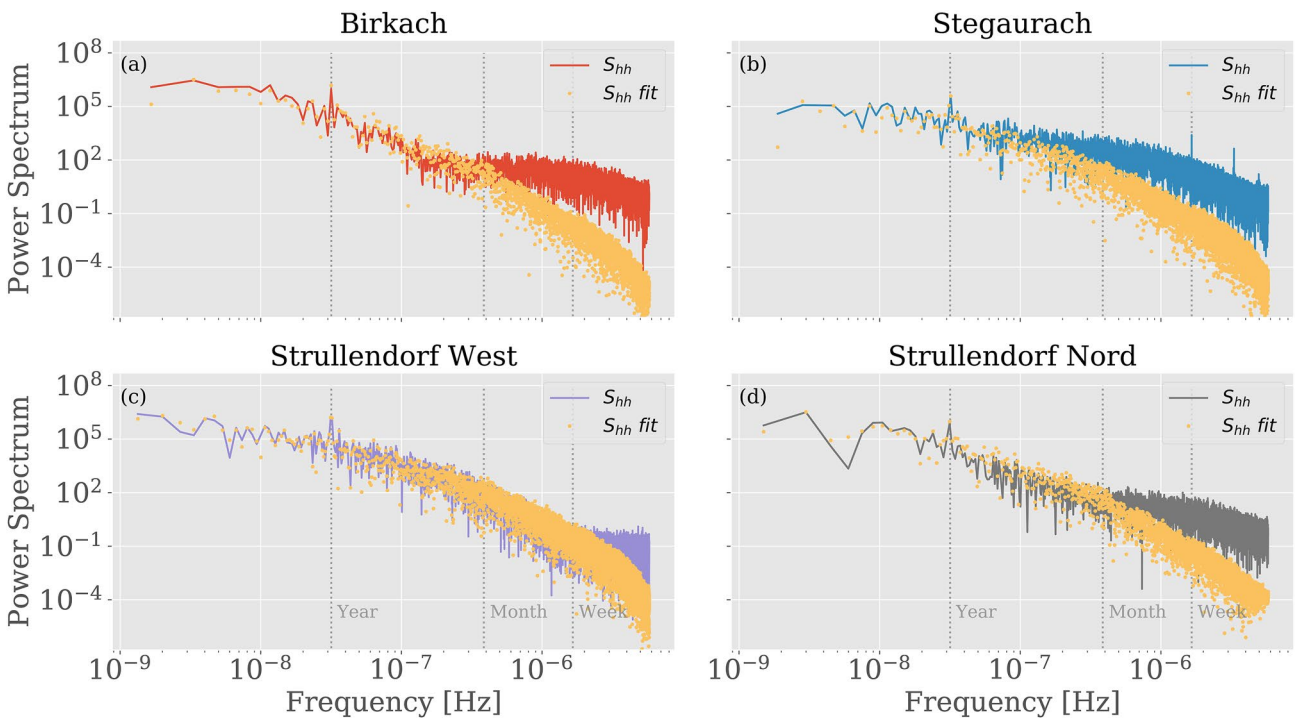

Figure 10. Spectra of groundwater levels (S_{hh}, solid) and a corresponding fit of the analytical solution (S_{hh} *fit*, dots) with the best R^2 value, selected from the analysis with manually estimated aquifer lengths based on geological expertise.

For *Strullendorf Nord* we robustly estimated all aquifer parameters (Table 1). Although the time series and the spectra of *Strullendorf Nord* and *Birkach* are relatively similar, the resulting characteristic times differ by a factor of 1.5.

6.5. Summary and Comprehensive Discussion

The spectra of the observed groundwater level fluctuations from the catchment in central Germany could be well fitted by the theoretical spectrum up to monthly time scales for at least three of the four investigated wells (*Birkach*, *Strullendorf West*, *Strullendorf Nord*, Figure 10).

For time scales below a month, the observed spectra diverge from the theoretical spectrum. A reason for the deviation might be monthly to weekly fluctuations in river height of the surrounding streams (e.g., the *Rauhe Ebrach*, south of *Birkach*, see supporting information for a hydrograph), the short term lateral inflow or highly fractured karstic materials which is not captured by the theoretical spectrum (Equation 8). Furthermore, the shape of the spectrum can be influenced by the superposition of local and intermediate flow systems, wetting and drying in partly saturated shallow aquifers (Zhang et al., 2022) as well as other hydrogeological processes.

Nevertheless, we clearly demonstrated that the characteristic time t_c as well as the storativity S could be robustly estimated using the spectral approach, that is, the results are only slightly sensitive to the aquifer length L and the position of the observation well x related to that length. In contrast, the estimated transmissivity T depends on a good estimate of the length L. If too little information about the aquifer is available and the aquifer length cannot be estimated it might be better to infer just the characteristic time. This parameter already allows to distinguish between different aquifer types and hydraulic regimes (Section 6.3).

In the second part of the field study, we estimated ranges for the length of the aquifer L and the related position of the observation well x with geological expertise, performed the spectral analysis, and obtained reasonable values. Since no additional information about the transmissivity and storativity of the aquifers could be acquired from literature, these results could not be compared and validated. Furthermore, estimates of T and S are often inferred from pumping, direct-push, slug tests, and laboratory tests. Considering the discussed regional information content of groundwater level time series and their spectra (representative, i.e., effective (Section 5.2) and equivalent (Section 5.3) aquifer parameters) compared to relatively local information from standard techniques (interpreted parameters) a direct comparison of these results might not be appropriate. Consequently, this study provides evidence that the spectral analysis might be a feasible methodology to bridge the scale and deliver averaged and regionally valid aquifer parameters. How large the representative volume of the aquifer characterized by the spectral analysis finally is, depends on the hydrogeological setting and its heterogeneity. Besides that, also topography, nested flow systems, and vertical hydraulic gradients will change the shape of the power spectra of hydraulic heads of different depths (Zhang et al., 2022). Consequently, the assumed Dupuit model may no longer be appropriate. Future studies in numerical environments will be specifically tailored to these research questions.

Even if the underlying concept of this methodology diverges from classical hydraulic tests, we consider an extensive comparison of the spectral analysis to existing methods as necessary and inevitable, which will be the scope of future studies as well. The synthetic study in this work including the application to real data should serve as a proof of concept in order to illustrate the methodology and its general feasibility.

Beside the investigation of L and x in well-known systems, we further need to evaluate the effect of temporally correlated recharge. While the synthetic experiments were driven by white noise recharge (uncorrelated), the real groundwater level time series were analyzed with a temporally correlated recharge extracted from an mHM model run. It has to be evaluated whether and under which circumstances the correlation time of the recharge signal interferes with the characteristic time of the aquifer influencing the results of the spectral analysis.

Additional complex synthetic studies as well as field studies with several observation wells, ideally drilled in aquifers with well-known properties, need to be conducted in order to compare the results and to tune the parameters of the spectral analysis.

The field data analysis supports the feasibility of the spectral approach and shows that this technique can be used to characterize the response of regional hydrological systems just by considering groundwater level and recharge time series as well as a rough estimate of the aquifer length and the position of the observation point.

7. Conclusion

In this study we investigated the feasibility of the spectral analysis in three synthetic model domains with different complexity (i.e., aquifer properties) and forcing. Finally, we examined the sensitivity of this approach by using real groundwater data recorded in the Main catchment in central Germany. We conclude this work with the following statements:

1. In synthetic, homogeneous environments, the model input parameters can be precisely derived with spectral analysis of groundwater level fluctuations as long as the time series are sufficiently long.
2. Time series of groundwater level fluctuation must be roughly 10 times as long as the characteristic time (aquifer response time) t_c of the aquifer. Consequently, short and higher conductive aquifers with small storativities are better suited for an investigation with the spectral analysis if observational periods are limited.
3. In stochastic ensembles of numerical models the effective transmissivity obtained from spectral analysis represents the geometric mean of the underlying distribution as long as the correlation length is small enough. The variance of the derived parameters is much smaller when the heads are observed in the aquifer body or close to the water divide.
4. Depending on the hydrogeological setting and the measurement location, the derived aquifer parameters are representative for local and/or regional portions of the aquifer. In settings where flow is forced to pass zones of lower hydraulic conductivity, the regional parameters are affected, while regions with high hydraulic conductivity seams to disappear, that is, having less effect on the hydraulic regime.
5. The sensitivity analysis has shown that even for different values of the position of the observation well x and the aquifer length L the resulting characteristic times are relatively similar. Consequently, the characteristic time can be robustly estimated with only little geologic information.
6. Field data analysis with the spectral approach granted reasonable results. Although complex flow regimes could be identified, the shape of the spectra follows the theoretical shape of a Dupuit aquifer at least for lower frequencies.
7. The characteristic time can be used in reservoir-type models where the groundwater compartment is represented in a conceptual way, while transmissivity and storativity values can be used in PDE-based models and converted to material properties (such as the hydraulic conductivity and specific storage) using the geometry (thickness) of the model.

The results of this work support the hypothesis that the spectrum of groundwater level fluctuations is mainly influenced by larger scale hydraulic properties. With that, spectral analysis might be a valuable method to infer regional hydraulic parameters from local groundwater measurements.

This tool can be used as a stand-alone procedure to estimate regionally valid aquifer properties or in combination with pumping tests to characterize the local properties as well. Future work will focus on a detailed validation, the identification of the aquifer length L as input parameter as well as the regionalization of the results of the spectral analysis with the help of auxiliary data sets.

Data Availability Statement

The groundwater simulations in this work were conducted with the open-source multi-physics software OpenGeoSys (OGS) version 5.7.1-49-g5255869 (Kolditz et al., 2012). The source code is written in C++ and can be downloaded from the corresponding GitHub repository (https://github.com/ufz/ogs5) together with additional tools for pre- and post-processing including the OGS Data Explorer. Heterogeneous stochastic hydraulic conductivity fields were generated and assigned to the grid cells with the combination of *ogs5py* (Müller, 2019) and *gstools* (Müller & Schüler, 2019). The complete geo-statistical framework can be accessed via https://geostat-framework.github.io/. Python scripts for model preparation, data processing, and analysis as well as for plotting are available on GitHub and Zenodo (Houben, 2022). Additional information can be found in Supporting Information S1 or directly in the repository. The modeled as well as the field data used for the spectral analysis in this study are available on Zenodo (Houben, 2021) with CC BY-NC. Please regard the included readme-file for additional license information.

Acknowledgments
This work was funded by the Helmholtz Centre for Environmental Research (UFZ) in Leipzig. The authors would like to thank three anonymous reviewers for constructive feedback which improved the quality of this paper. Furthermore, we thank Rohini Kumar for providing the mHM recharge time series, Falk Hesse and Sebastian Müller for support with the stochastic analysis as well as for help with the model setup. Thanks to Lennart Schüler for mathematical support concerning the analytical solutions and Fanny Sarrazin for providing concepts for the sensitivity analysis. We would like to thank the group of the groundwater initiative at UFZ, especially Christian Siebert and Tino Rödiger for constructive feedback about the results of the spectral analysis, the selection of the groundwater wells, and corresponding data sets. The scientific results have been computed at the High-Performance Computing (HPC) Cluster EVE, a joint effort of both the Helmholtz Centre for Environmental Research - UFZ (http://www.ufz.de/) and the German Centre for Integrative Biodiversity Research (iDiv) Halle-Jena-Leipzig (http://www.idiv-biodiversity.de/). E. Pujades and S. Attinger greatfully acknowledge the support from the research initiative Global Resource Water (GRoW; 02WGR1423A-F). GRoW is part of the Sustainable Water Management (NaWaM) funding priority within the Research for Sustainable Development (FONA) framework of the German Federal Ministry of Education and Research (BMBF). E. Pujades acknowledges the financial support from IDAEA-CSIC, which is a Centre of Excellence Severo Ochoa (Spanish Ministry of Science and Innovation, Project CEX2018-000794-S), and the Barcelona City Council through the Award for Scientific Research into Urban Challenges in the City of Barcelona 2020 (20S08708). Open access funding enabled and organized by Projekt DEAL.

References

Bakr, A. A., Gelhar, L. W., Gutjahr, A. L., & MacMillan, J. R. (1978). Stochastic analysis of spatial variability in subsurface flows: 1. Comparison of one- and three-dimensional flows. *Water Resources Research*, *14*(2), 263–271. https://doi.org/10.1029/wr014i002p00263

Bear, J. (1972). *Dynamics of fluids in porous media*. New York: American Elsevier Pub. Co. https://doi.org/10.1097/00010694-197508000-00022

Butler, J. J., Dietrich, P., Wittig, V., & Christy, T. (2007). Characterizing hydraulic conductivity with the direct-push permeameter. *Ground Water*, *45*(4), 409–419. https://doi.org/10.1111/j.1745-6584.2007.00300.x

Butler, J. J., Gomez-Hernandez, J. J., Perrone, D., & Hyndman, D. W. (2021). Introduction to special section: The quest for sustainability of heavily stressed aquifers at regional to global scales. *Water Resources Research*, *57*(8). https://doi.org/10.1029/2021wr030446

Carr, E. J., & Simpson, M. J. (2018). Accurate and efficient calculation of response times for groundwater flow. *Journal of Hydrology*, *558*, 470–481. https://doi.org/10.1016/j.jhydrol.2017.12.023

Condon, L. E., & Maxwell, R. M. (2014). Groundwater-fed irrigation impacts spatially distributed temporal scaling behavior of the natural system: A spatio-temporal framework for understanding water management impacts. *Environmental Research Letters*, *9*(3), 034009. https://doi.org/10.1088/1748-9326/9/3/034009

Dagan, G. (1979). Models of groundwater flow in statistically homogeneous porous formations. *Water Resources Research*, *15*(1), 47–63. https://doi.org/10.1029/wr015i001p00047

de Marsily, G., Delay, F., Gonçalvès, J., Renard, P., Teles, V., & Violette, S. (2005). Dealing with spatial heterogeneity. *Hydrogeology Journal*, *13*(1), 161–183. https://doi.org/10.1007/s10040-004-0432-3

de Rooij, G. H. (2012). Transient flow between aquifers and surface water: Analytically derived field-scale hydraulic heads and fluxes. *Hydrology and Earth System Sciences*, *16*(3), 649–669. https://doi.org/10.5194/hess-16-649-2012

de Rooij, G. H. (2013). Aquifer-scale flow equations as generalized linear reservoir models for strip and circular aquifers: Links between the Darcian and the aquifer scale. *Water Resources Research*, *49*(12), 8605–8615. https://doi.org/10.1002/2013wr014873

Desbarats, A. J., & Srivastava, R. M. (1991). Geostatistical characterization of groundwater flow parameters in a simulated aquifer. *Water Resources Research*, *27*(5), 687–698. https://doi.org/10.1029/90wr02705

Dietrich, P., & Leven, C. (2009). Direct push-technologies. In K. R. (Ed.), *Groundwater geophysics* (pp. 347–366). Springer. https://doi.org/10.1007/978-3-540-88405-7_12

Erskine, A., & Papaioannou, A. (1997). The use of aquifer response rate in the assessment of groundwater resources. *Journal of Hydrology*, *202*(1–4), 373–391. https://doi.org/10.1016/s0022-1694(97)00058-9

Fleming, S. W., Lavenue, A. M., Aly, A. H., & Adams, A. (2002). Practical applications of spectral analysis to hydrologic time series. *Hydrological Processes*, *16*(2), 565–574. https://doi.org/10.1002/hyp.523

Freeze, R. (1979). *Groundwater*. Englewood Cliffs, NJ: Prentice-Hall.

Gelhar, L. W. (1974). Stochastic analysis of phreatic aquifers. *Water Resources Research*, *10*(3), 539–545. https://doi.org/10.1029/wr010i003p00539

Gelhar, L. W., & Wilson, J. L. (1974). Ground-water quality modeling. *Ground Water*, *12*(6), 399–408. https://doi.org/10.1111/j.1745-6584.1974.tb03050.x

Gutjahr, A. L., Gelhar, L. W., Bakr, A. A., & MacMillan, J. R. (1978). Stochastic analysis of spatial variability in subsurface flows: 2. Evaluation and application. *Water Resources Research*, *14*(5), 953–959. https://doi.org/10.1029/wr014i005p00953

Hamman, J. J., Nijssen, B., Bohn, T. J., Gergel, D. R., & Mao, Y. (2018). The variable infiltration capacity model version 5 (VIC-5): Infrastructure improvements for new applications and reproducibility. *Geoscientific Model Development*, *11*(8), 3481–3496. https://doi.org/10.5194/gmd-11-3481-2018

Hellwig, J., Graaf, I. E. M., Weiler, M., & Stahl, K. (2020). Large-scale assessment of delayed groundwater responses to drought. *Water Resources Research*, *56*(2). https://doi.org/10.1029/2019wr025441

Henningsen, D., & Katzung, G. (2011). *Einführung in die geologie deutschlands*. Spektrum-Akademischer Vlg.

Houben, T. (2021). *Data bundle for houben et al. (2022) - spectral analysis of gw level measurements [collection]*. https://doi.org/10.5281/ZENODO.5525001

Houben, T. (2022). Github repository: timohouben/houben_spectral_analysis: V1.0 - final release, python scripts for spectral analysis. [software]. Zenodo. https://doi.org/10.5281/ZENODO.6139557

Jiménez-Martínez, J., Longuevergne, L., Borgne, T. L., Davy, P., Russian, A., & Bour, O. (2013). Temporal and spatial scaling of hydraulic response to recharge in fractured aquifers: Insights from a frequency domain analysis. *Water Resources Research*, *49*(5), 3007–3023. https://doi.org/10.1002/wrcr.20260

Jing, M., Heße, F., Kumar, R., Wang, W., Fischer, T., Walther, M., et al. (2018). Improved regional-scale groundwater representation by the coupling of the mesoscale hydrologic model (mHM v5.7) to the groundwater model OpenGeoSys (OGS). *Geoscientific Model Development*, *11*(5), 1989–2007. https://doi.org/10.5194/gmd-11-1989-2018

Khintchine, A. (1934). Korrelationstheorie der stationaeren stochastischen prozesse. *Mathematische Annalen*, *109*(1), 604–615. https://doi.org/10.1007/bf01449156

Kolditz, O., Bauer, S., Bilke, L., Böttcher, N., Delfs, J. O., Fischer, T., et al. (2012). OpenGeoSys: An open-source initiative for numerical simulation of thermo-hydro-mechanical/chemical (THM/c) processes in porous media. *Environmental Earth Sciences*, *67*(2), 589–599. https://doi.org/10.1007/s12665-012-1546-x

Kumar, R., Samaniego, L., & Attinger, S. (2013). Implications of distributed hydrologic model parameterization on water fluxes at multiple scales and locations. *Water Resources Research*, *49*(1), 360–379. https://doi.org/10.1029/2012wr012195

Liang, X., & Zhang, Y.-K. (2013). Temporal and spatial variation and scaling of groundwater levels in a bounded unconfined aquifer. *Journal of Hydrology*, *479*, 139–145. https://doi.org/10.1016/j.jhydrol.2012.11.044

Liang, X., & Zhang, Y.-K. (2015). Analyses of uncertainties and scaling of groundwater level fluctuations. *Hydrology and Earth System Sciences*, *19*(7), 2971–2979. https://doi.org/10.5194/hess-19-2971-2015

Manga, M. (1999). On the timescales characterizing groundwater discharge at springs. *Journal of Hydrology*, *219*(1–2), 56–69. https://doi.org/10.1016/s0022-1694(99)00044-x

Markovic, D., & Koch, M. (2014). Stream response to precipitation variability: A spectral view based on analysis and modelling of hydrological cycle components. *Hydrological Processes*, *29*(7), 1806–1816. https://doi.org/10.1002/hyp.10293

Markstrom, S. L., Niswonger, R. G., Regan, R. S., Prudic, D. E., & Barlow, P. M. (2005). *Gsflow—Coupled ground-water and surface-water flow model based on the integration of the Precipitation-Runoff Modeling System (PRMS) and the Modular Ground-Water Flow Model (MODFLOW-2005)*. U.S. Geological Survey.

Maxwell, R. M., & Miller, N. L. (2005). Development of a coupled land surface and groundwater model. *Journal of Hydrometeorology*, *6*(3), 233–247. https://doi.org/10.1175/jhm422.1

Molénat, J., Davy, P., Gascuel-Odoux, C., & Durand, P. (1999). Study of three subsurface hydrologic systems based on spectral and cross-spectral analysis of time series. *Journal of Hydrology*, *222*(1–4), 152–164. https://doi.org/10.1016/s0022-1694(99)00107-9

Molénat, J., Davy, P., Gascuel-Odoux, C., & Durand, P. (2000). Spectral and cross-spectral analysis of three hydrological systems. *Physics and Chemistry of the Earth - Part B: Hydrology, Oceans and Atmosphere*, *25*(4), 391–397. https://doi.org/10.1016/s1464-1909(00)00032-0

Müller, S. (2019). ogs5py v1.0.5 (v1.0.5). [Software]. Zenodo. https://doi.org/10.5281/ZENODO.3546035

Müller, S., & Schüler, L. (2019). Geostat-framework/gstools: Bouncy blue. [Software]. Zenodo. https://doi.org/10.5281/ZENODO.2543658

Pechstein, A., & Copty, N. K. (2021). Interpretation of pumping tests in heterogeneous aquifers with constant head boundary. *Groundwater*, *59*(4), 517–523. https://doi.org/10.1111/gwat.13072

Rousseau-Gueutin, P., Love, A. J., Vasseur, G., Robinson, N. I., Simmons, C. T., & deMarsily, G. (2013). Time to reach near-steady state in large aquifers. *Water Resources Research*, *49*(10), 6893–6908. https://doi.org/10.1002/wrcr.20534

Russian, A., Dentz, M., Borgne, T. L., Carrera, J., & Jimenez-Martinez, J. (2013). Temporal scaling of groundwater discharge in dual and multi-continuum catchment models. *Water Resources Research*, *49*(12), 8552–8564. https://doi.org/10.1002/2013wr014255

Russo, T. A., & Lall, U. (2017). Depletion and response of deep groundwater to climate-induced pumping variability. *Nature Geoscience*, *10*(2), 105–108. https://doi.org/10.1038/ngeo2883

Samaniego, L., Kumar, R., & Attinger, S. (2010). Multiscale parameter regionalization of a grid-based hydrologic model at the mesoscale. *Water Resources Research*, *46*(5). https://doi.org/10.1029/2008wr007327

Sanchez-Vila, X., Guadagnini, A., & Carrera, J. (2006). Representative hydraulic conductivities in saturated groundwater flow. *Reviews of Geophysics*, *44*(3). https://doi.org/10.1029/2005rg000169

Schilling, K. E., & Zhang, Y.-K. (2011). Temporal scaling of groundwater level fluctuations near a stream. *Ground Water*, *50*(1), 59–67. https://doi.org/10.1111/j.1745-6584.2011.00804.x

Schneider, C. L., & Attinger, S. (2008). Beyond Thiem: A new method for interpreting large scale pumping tests in heterogeneous aquifers. *Water Resources Research*, *44*(4). https://doi.org/10.1029/2007wr005898

Schuite, J., Flipo, N., Massei, N., Rivière, A., & Baratelli, F. (2019). Improving the spectral analysis of hydrological signals to efficiently constrain watershed properties. *Water Resources Research*, *55*(5), 4043–4065. https://doi.org/10.1029/2018wr024579

Smith, L., & Freeze, R. A. (1979). Stochastic analysis of steady state groundwater flow in a bounded domain - 1. One-dimensional simulations. *Water Resources Research*, *15*(3), 521–528. https://doi.org/10.1029/wr015i003p00521

Srivastava, V., Graham, W., Muñoz-Carpena, R., & Maxwell, R. M. (2014). Insights on geologic and vegetative controls over hydrologic behavior of a large complex basin – Global sensitivity analysis of an integrated parallel hydrologic model. *Journal of Hydrology*, *519*, 2238–2257. https://doi.org/10.1016/j.jhydrol.2014.10.020

Sutanudjaja, E. H., van Beek, L. P. H., de Jong, S. M., van Geer, F. C., & Bierkens, M. F. P. (2011). Large-scale groundwater modeling using global datasets: A test case for the Rhine-Meuse basin. *Hydrology and Earth System Sciences*, *15*(9), 2913–2935. https://doi.org/10.5194/hess-15-2913-2011

Sutanudjaja, E. H., van Beek, R., Wanders, N., Wada, Y., Bosmans, J. H. C., Drost, N., et al. (2018). PCR-GLOBWB 2: A 5 arcmin global hydrological and water resources model. *Geoscientific Model Development*, *11*(6), 2429–2453. https://doi.org/10.5194/gmd-11-2429-2018

van de Leur, D. A. K. (1958). A study of non-steady groundwater flow with special reference to a reservoir-coefficient. *De Ingenieur*, *70*(19), 87–94. Retrieved from https://edepot.wur.nl/422032

Whittemore, D. O., Butler, J. J., & Wilson, B. B. (2015). Assessing the major drivers of water-level declines: New insights into the future of heavily stressed aquifers. *Hydrological Sciences Journal*, *61*(1), 134–145. https://doi.org/10.1080/02626667.2014.959958

Wiener, N. (1930). Generalized harmonic analysis. *Acta Mathematica*, *55*(0), 117–258. https://doi.org/10.1007/bf02546511

Wilkinson, W. B., & Cooper, D. M. (1993). The response of idealized aquifer/river systems to climate change. *Hydrological Sciences Journal*, *38*(5), 379–390. https://doi.org/10.1080/026266693099492688

Zhang, X., Li, H., J, J. J., Luo, X., Kuang, X., Mao, R., & Hu, W. (2022). Fractal behaviors of hydraulic head and surface runoff of the nested groundwater flow systems in response to rainfall fluctuations. *Geophysical Research Letters*, *49*(2). https://doi.org/10.1029/2021gl093784

Zhang, Y.-K., & Li, Z. (2005). Temporal scaling of hydraulic head fluctuations: Nonstationary spectral analyses and numerical simulations. *Water Resources Research*, *41*(7). https://doi.org/10.1029/2004wr003797

Zhang, Y.-K., & Li, Z. (2006). Effect of temporally correlated recharge on fluctuations of groundwater levels. *Water Resources Research*, *42*(10). https://doi.org/10.1029/2005wr004828

Zhang, Y.-K., & Schilling, K. (2004). Temporal scaling of hydraulic head and river base flow and its implication for groundwater recharge. *Water Resources Research*, *40*(3). https://doi.org/10.1029/2003wr002094

Zhang, Y.-K., & Schilling, K. (2005). Temporal variations and scaling of streamflow and baseflow and their nitrate-nitrogen concentrations and loads. *Advances in Water Resources*, *28*(7), 701–710. https://doi.org/10.1016/j.advwatres.2004.12.014

Zhang, Y.-K., & Yang, X. (2010). Effects of variations of river stage and hydraulic conductivity on temporal scaling of groundwater levels: Numerical simulations. *Stochastic Environmental Research and Risk Assessment*, *24*(7), 1043–1052. https://doi.org/10.1007/s00477-010-0437-5

Zink, M., Kumar, R., Cuntz, M., & Samaniego, L. (2017). A high-resolution dataset of water fluxes and states for Germany accounting for parametric uncertainty. *Hydrology and Earth System Sciences*, *21*(3), 1769–1790. https://doi.org/10.5194/hess-21-1769-2017